

Switching-like event-triggered tracking control for UAH/UGV systems under external disturbance and DoS attacks

Tao Li¹, Haoran Zhang¹, Shihao Pan¹, and Zehui Mao¹

¹Nanjing University of Aeronautics and Astronautics College of Automation Engineering

April 15, 2023

Abstract

In this paper, by considering the existence of unavailable state, external disturbance, and denial of service (DoS) attacks, an anti-disturbance trajectory tracking controller is proposed for the air-ground system composed of unmanned autonomous helicopter (UAH) and unmanned ground vehicle (UGV). Initially, by combining the advantages of conventional event-triggered scheme (ETS) and memory ETS, a switching-like event-triggered mechanism is put forward, which can cause less data transmissions without reducing control performance, and effectively restrain the DoS attacks. Secondly, by dividing the DoS attacks into active intervals and sleep ones, the concept of acknowledgement character technology (ACK) is presented to determine the suitable type of time intervals. Thirdly, the switching-like dynamic ETS is introduced for the sleep intervals of DoS attacks while the ETS with fixed triggered-threshold is exploited for the active intervals. Fourthly, based on the occurrence of the DoS attacks, a switching-like observer and a normal one are respectively proposed to estimate the UGV state, the UAH state, the reference input of the UGV, and the disturbance of the UAH, which are utilized to design the anti-disturbance tracking controller. Fifthly, an augmented closed-loop system consisting of observation errors and tracking error is established and its stability is analyzed by using Lyapunov stability theory. Then, a sufficient condition on co-designing the parameters of switching-like ETS, observers, and tracking controller is presented in terms of linear matrix inequalities (LMI). Finally, the validity and superiority of the proposed control scheme are verified by resorting to simulations and comparisons.

RESEARCH ARTICLE

Switching-like event-triggered tracking control for UAH/UGV systems under external disturbance and DoS attacks

Haoran Zhang | Shihao Pan | Tao Li* | Zehui Mao

School of Automation Engineering, Nanjing University of Aeronautics and Astronautics, Nanjing 211106, Jiangsu, PR China

Correspondence

Tao Li. Email: autolitao@nuaa.edu.cn

Present Address

School of Automation Engineering, Nanjing University of Aeronautics and Astronautics, Nanjing 211106, Jiangsu, PR China

Summary

In this paper, by considering the existence of unavailable state, external disturbance, and denial of service (DoS) attacks, an anti-disturbance trajectory tracking controller is proposed for the air-ground system composed of unmanned autonomous helicopter (UAH) and unmanned ground vehicle (UGV). Initially, by combining the advantages of conventional event-triggered scheme (ETS) and memory ETS, a switching-like event-triggered mechanism is put forward, which can cause less data transmissions without reducing control performance, and effectively restrain the DoS attacks. Secondly, by dividing the DoS attacks into active intervals and sleep ones, the concept of acknowledgement character technology (ACK) is presented to determine the suitable type of time intervals. Thirdly, the switching-like dynamic ETS is introduced for the sleep intervals of DoS attacks while the ETS with fixed triggered-threshold is exploited for the active intervals. Fourthly, based on the occurrence of the DoS attacks, a switching-like observer and a normal one are respectively proposed to estimate the UGV state, the UAH state, the reference input of the UGV, and the disturbance of the UAH, which are utilized to design the anti-disturbance tracking controller. Fifthly, an augmented closed-loop system consisting of observation errors and tracking error is established and its stability is analyzed by using Lyapunov stability theory. Then, a sufficient condition on co-designing the parameters of switching-like ETS, observers, and tracking controller is presented in terms of linear matrix inequalities (LMI). Finally, the validity and superiority of the proposed control scheme are verified by resorting to simulations and comparisons.

KEYWORDS:

unmanned autonomous helicopter (UAH), unmanned ground vehicle (UGV), denial of service (DoS) attacks, switching-like event-trigger, trajectory tracking control

1 | INTRODUCTION

The UAH is the most common aircraft, and possesses many advantages such as vertical landing, hovering in the air, and in-place turning¹⁻³. Thus, in recent years, the UAH has stood out among many aircrafts, and been widely utilized in many civil and military fields including high-altitude patrol, intelligence collection, warship operation, precision agriculture and disaster monitoring^{4,5}. Meanwhile, the UGV also plays an important role in ground transportation, reconnaissance, navigation, and

⁰Abbreviations: UAH, UGV, denial of service attacks, switching-like event-trigger, trajectory tracking control

patrolling⁶. Together with rapid developments of science and technology, the applications of the UAH in national defense and general aviation have been widely reported. However, due to the increasing requirements, the UAH can no longer complete tasks independently, and it needs to work with the UGV as air-ground cooperative control to tackle more complex environments. The UGV provides the track reference and supplies for the UAH, which needs communication network to interact with the UGV. Then, the core of air-ground cooperative control is trajectory tracking control⁷⁻¹³. In⁹, the cooperative control for the UAH/UGV systems was studied with the constraints of the UGV speed, the load power of the UAH, and the communication restrictions between the UAH and the UGV. Aiming at the different structures of the UAH and the UGV, in¹⁰, a new comprehensive heterogeneous multi-agent systems dynamics model was established and a distributed fault-tolerant time-varying formation control method under unknown faults and external disturbances was proposed. In¹¹, an air-ground cooperative control scheme for the UAHs and UGVs equipped with multiple cameras was designed to complete some visual tracking tasks. The UAH was used to assist the UGV to achieve accurate positioning¹² and the UGV tracking the UAH steady was performed with visual information¹³. However, since the UAH and the UGV need communication network to transmit the data of position and velocity, these above studies considered the ideal case and ignored some unfavorable factors such as resource limitations, cyber-attacks, and so on. To name a few, the Ref.¹⁴, a trajectory control scheme based on hybrid ETS was proposed for UAH/UGV systems subject to time-delay, external disturbance, and deception attacks. It is worth noting that since DoS attacks prevent data packets from being transmitted via the network, this kind of cyber-attack would heavily ruin the tracking control performance for the UAH/UGV systems, which remains important and challenging.

In recent years, by reducing the number of data transmissions, the ETS has been verified to be effective in solving communication constraints and received much research attention, which was widely utilized and improved¹⁵⁻²⁵. For instance, in¹⁶, two separate static ETSs were designed to trigger sampled signals from sensor to controller and from controller to actuator, respectively. In¹⁸, an ETS with time-delay was presented to handle the static output feedback control of networked control systems (NCSs). Yet, in¹⁵⁻¹⁸, the triggering thresholds are preset constants and cannot reflect real-time control performance. Then, the adaptive ETS and dynamic ETS were presented, and their thresholds were dynamically adjustable, which could be more efficient than the ETS with fixed-thresholds. By modeling an outside systems to adjust triggering thresholds, a dynamic ETS in¹⁹ was presented to design the synchronization controllers for discrete-time complex networks, and in²⁰, a dynamic ETS was utilized from controller to executor to reduce bandwidth usage and executor action frequency. In²¹, an adaptive ETS was proposed to tackle the progress of fault detection and the probability of fault occurrence, in which the triggering threshold was adjusted by the state. It is worth noting that these above ETSs including adaptive and dynamic cases only aimed to how to reduce data transmissions as much. Normally, together with less data transmissions, the control performance would be decreased accordingly. In order to overcome this shortcoming, a new ETS called memory ETS was put forward in²² and it could include multiple historically transmitted data endowed with different weights. This kind of memory ETS could not only reduce the data transmissions, but also help to reject disturbance and achieve desirable performance²²⁻²⁵, which was widely investigated in most recent years. Especially, in²³, the adaptive triggering thresholds in memory ETS were used to instead of fixed ones to better realize real-time control performance. In²⁴, a window function was proposed to reasonably assign weight values to recently transmitted data, and the memory ETS could deal with the continuous system. Similarly, in²⁵, some adjustable triggered thresholds were added into the memory ETS to execute security filters. As illustrated in²³, the memory ETS is less effective than the conventional ones in¹⁵⁻²¹ in reduce data transmissions. Thus, the Ref.¹⁴ proposed a hybrid ETS to decrease the number of transmitted data and achieve ideal control performance, which could combine the advantages of conventional ETS and memory ETS. Yet, as for network-based control systems, it is required that not only less data transmissions but also cyber-attacks need to be considered. Then the hybrid ETS in¹⁴ cannot simultaneously tackle these unfavorable factors in some complicated cases, which motivates this paper to propose a design of switching-like ETS.

Normally, under the network environments, the cyber-attacks bring great challenges when the ETS and controller are designed altogether, among which the DoS attacks are most common. Based on^{26,27}, such cyber-attack may prevent the data packets from being transmitted via the network, resulting in poor performance or even instability. Owing to harmfulness, many effective techniques have been proposed to tackle the DoS attacks including the event-trigger one. For instance, under event-triggered control framework, an observer with adjustable gains was constructed to compensate for the aperiodic DoS attacks actively²⁸. In²⁹, a switching-like controller with variable gains was proposed to handle DoS attacks and disturbance in NCSs. Based on designing the ETS, in³⁰, a resilient dynamic ETS was proposed against two-channel DoS attacks and transmission delay was involved. In³¹, by using a discrete-time model to describe the DoS attacks, two static ETSs with different thresholds were designed to switch the situations where the DoS attacks occur or not. In³², a model free adaptive controller was proposed based

on ETS for nonlinear NCSs subjected to sensor failures and DoS attacks. By considering dual-terminal DoS attacks and time-delays, the switching rate was used to design the ETS to cope with the switching system³³. Meanwhile, as for the tracking control for UAH/UGV systems, owing to complex circumstances, on one hand, the UAH is unavoidably affected by the gusts and its size is sensitive to outside disturbance; on the other hand, owing to that the UGV information needs to be transmitted to the UAH via communication network, these data may suffer from the cyber-attacks including the DoS attacks. Especially, in comparison with other cyber-attacks, the DoS attacks are much more difficult to be tackled owing to complex characteristics and harmfulness. Up to now, few works have investigated the event-triggered trajectory tracking control for the UAH/UGV systems under outside disturbance, resource restraint, and DoS attacks, which constitutes the focus of this presented paper.

Motivated by above discussions, by combing the advantages of existent ETSs and characteristics of DoS attacks, a new type of switching-like ETS is proposed, and an anti-disturbance tracking control scheme is established for the UAH/UGV systems under outside disturbance. The contributions of this paper are summarized as follows:

1. During modeling the DoS attacks, the ACK concept is initially introduced to determine whether such attack remains in active interval and sleep one. Then, as for sleep interval, a switching-like ETS with dynamic thresholds is proposed to jointly realize less data transmissions and ideal control performance, while in active one, an ETS with the fixed threshold is presented to improve communication efficiency. In comparison with some other ETSs, our event-triggered mechanism can be more effective in tackling the packet losses by DoS attacks and resource constraint.
2. Based on the tracking control target and occurring intervals of DoS attacks, a switching-like observer in the UAH system is proposed to estimate the state and reference signal of UGV system, and a normal observer is put forward to obtain the estimations of the disturbance and state of UAH system. Together with the observations, tracking error, and DoS attacks, an anti-disturbance switching tracking controller is exploited to derive an augmented closed-loop system.
3. By resorting to Lyapunov stability theory, a sufficient condition is derived to ensure the bounded stability for the derived closed-loop system. Moreover, by exploiting suitable matrix techniques, a co-design method of checking the triggering parameters, observer gains, and controller gains is provided in the form of the LMIs, which can be easily tested and applied to the air-ground tracking control for real UAH/UGV systems.

The rest of this paper is structured in what follows. In section 2, some preparations for the problem and the establishment of models are described. Section 3 provides the main results, including the maximum allowable condition for DoS attacks, uniform ultimate boundedness conditions for augmented closed-loop system, and the methods for designing the controller. In section 4, two different simulated experiments are given to demonstrate the effectiveness and superiority of the proposed scheme. Finally, the conclusion is given in Section 5.

Notations: The term $\mathbb{R}^{n \times m}$ is the set of $n \times m$ constant matrices, \mathbb{N} and $\mathbb{N}_{\geq 0}$ represent non-negative and positive integers respectively. I_n is the identity matrix of $n \times n$ dimensions, and 0 denotes the zero matrix with appropriate dimensions. Given a vector x , \hat{x} is the estimated value of x , x^T represents the transposition of x . For a matrix A , A^T denotes the transposition of A , A^{-1} is the inverse of a non-singular matrix A , $\|A\|$ represents the Euclidean norm of A , and $\lambda_{\max}(A)$ means the maximum eigenvalues of A . In addition, $\text{He}(X) = X + X^T$ and $*$ stands for the symmetric items in one matrix.

2 | PROBLEM FORMULATIONS AND MODELING

The main purpose of air-ground trajectory tracking control can be described as that the UGV generates its own motion path according to reference signal, and transmits the information to the UAH via communication network, which can make the UAH tracks the UGV according to received information. In this section, the linear models of the UGV and UAH are presented in Section 2.1, the switching-like ETS under the DoS attacks is represented in Section 2.2, the state observer and disturbance one of the UGV and UAH are given in Section 2.3, and the trajectory tracking controller of UAH is shown in Section 2.4.

2.1 | Model descriptions of UAH/UGV systems

Based on the Refs.^{34, 35}, the dynamics of the UAH and UGV systems to be controlled are respectively presented by the following linear discrete-time equations

$$\text{UGV system : } \begin{cases} x_a(k+1) = A_a x_a(k) + B_a u_a(k) + B_r r(k), \\ y_a(k) = C_a x_a(k), \end{cases} \quad (1)$$

$$\text{UAH system : } \begin{cases} x_b(k+1) = A_b x_b(k) + B_b u_b(k) + B_d d(k), \\ y_b(k) = C_b x_b(k), \end{cases} \quad (2)$$

where $x_a(k) = [x_{ax}(k), x_{ay}(k)]^T \in \mathbb{R}^{2 \times 1}$ and $x_b(k) = [x_{bx}(k), v_{bx}(k), x_{by}(k), v_{by}(k)]^T \in \mathbb{R}^{4 \times 1}$ represent the position and velocity states of the UAH/UGV system, $u_a(k) \in \mathbb{R}^{2 \times 1}$ and $u_b(k) \in \mathbb{R}^{2 \times 1}$ mean the control inputs of the UAH/UGV systems, $y_a(k) \in \mathbb{R}^{2 \times 1}$ and $y_b(k) \in \mathbb{R}^{2 \times 1}$ are the measurement outputs of the UAH/UGV systems, $r(k) \in \mathbb{R}^{2 \times 1}$ is the given reference input and $d(k) \in \mathbb{R}^{u \times 1}$ means the disturbance. In addition, $A_a, A_b, B_a, B_b, C_a, C_b, B_r, B_d$ are the known matrices with appropriate dimensions.

Remark 1. Since the position information is transmitted from the UGV to the UAH, the UGV system can be regarded as a planar two-dimensional motion. Even if there is a change in height, it can be reasonably ignored. Similarly, the speed of the UGV is not considered in this paper. For the UAH system, a new event mechanism proposed in this paper focuses on how to design an effective ETS to decrease the number of transmitted data and maintain desirable tracking performance as much when the UAH system is attacked by the DoS attack. Therefore, it can be assumed that the UAH is moving in hovering flight condition, that is, it does not consider the change of its attitude during the flight in order to clearly illustrate the main research of this paper.

The following assumption is used to describe the reference input $r(k)$ and the disturbance $d(k)$ for the designs of observer and controller, and the other one is placed on the establishment of the tracking error system.

Assumption 1. The discrete-time equations of the reference input $r(k)$ and the disturbance $d(k)$ satisfy $r(k+1) = r(k) + \Delta r(k)$ and $d(k+1) = d(k) + \Delta d(k)$. In addition, there exists a relationship between $r(k)$ and $x_a(k)$, i.e., $\|r(k)\| \leq \eta \|x_a(k)\|$, η is a positive constant. Suppose there exist two positive constants o_1, o_2 such that $r(k)$ and $d(k)$ are norm-bounded, that is to say, $\|r(k)\| \leq o_1$, $\|d(k)\| \leq o_2$. Similarly, there are two positive constants o_3, o_4 such that $\Delta r(k)$ and $\Delta d(k)$ are norm-bounded, that is to say, $\|\Delta r(k)\| \leq o_3$, $\|\Delta d(k)\| \leq o_4$.

Assumption 2.³⁶ On one hand, the states of UAH/UGV systems one are unmeasurable. On the other hand, for the parameters in the UAH/UGV systems, $\text{rank}(B_b) = \text{rank}(B_b, B_d)$ holds, and there exist the matrices S, H_1, H_2, H_3 and H_4 satisfying $SA_b + SB_b H_1 = (A_a + B_a H_2)S$, $SB_b H_3 = B_r$ and $SB_b H_4 = SB_d$.

Then, since the UGV state is not measurable, a static output feedback controller is proposed as follows:

$$u_a(k) = K_a y_a(k). \quad (3)$$

Therefore, the UAH system in (1) is rewritten as

$$\begin{cases} x_a(k+1) = (A_a + B_a K_a C_a) x_a(k) + B_r r(k), \\ y_a(k) = C_a x_a(k). \end{cases} \quad (4)$$

Remark 2. The parameter K_a in (3) needs to meet the restriction that all eigenvalues of the matrix $A_a + B_a K_a C_a$ in (4) are in the unit circle, such that system (4) can be bounded stable according to Assumption 1.

The framework of the whole air-ground tracking control is schematically described in Fig. 1. From Fig. 1, since the communicate network is involved between the UGV and the UAH, then the UAH needs to estimate the UGV state based on the composite signal composed of $y_a(k)$ and $r(k)$ transmitted by the UGV system. The composite signal is defined as $\varrho_y(k) = [y_a^T(k), r^T(k)]^T$. In order to save communication resource and tackle the random DoS attacks, a switching-like ETS is proposed on the basis of the advantages of existent ETSs. At the same time, the proposed ETS in the UAH system can reduce the subsequent signal transmissions. Based on the signal value obtained at the triggered time, an observer in the UAH system is established to estimate the state and reference input of the UGV. The UAH state and the interference it receives can be observed without the need of triggering time signal, so as used to complete the trajectory tracking controller design.

2.2 | Design of switching-like ETS under DoS attacks

In order to better describe the design idea of the switching-like ETS of this paper, a new vector is designed to represent the composed signal as follows

$$\tilde{\varrho}_y(k) = \sum_{i=0}^{m-1} p_i \varrho_y(k-i) = [\tilde{y}_a^T(k), \tilde{r}^T(k)]^T, \quad (5)$$

where p_i ($i = 0, 1, \dots, m-1$) are the weights that satisfy $\sum_{i=0}^{m-1} p_i = 1$, and $p_i \in [0, 1]$.

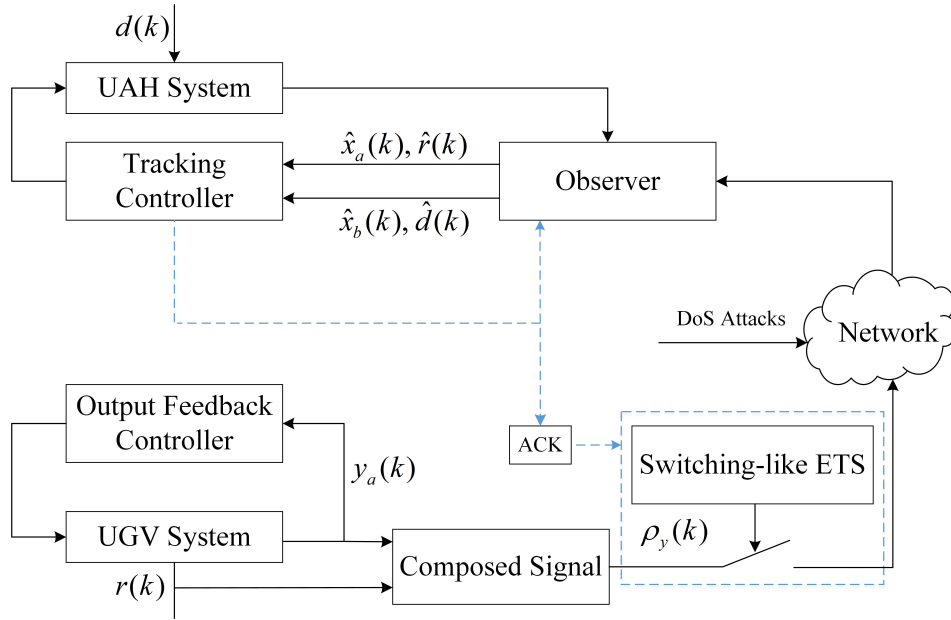


FIGURE 1 The structure of the air-ground tracking control of UAH/UGV systems.

Suppose that the sampling sequence is $\mathcal{N}_1 = \{0, h, 2h, \dots, kh, \dots\}$, $k \in \mathbb{N}$, where h is the sampling period. Based the Refs.²⁸ and³⁸, by collecting the sampled information, a switching-like ETS communication scheme is designed as

$$t_{k+1} = \begin{cases} \text{Memory ETS : } \min_{k \in \mathbb{N}} \left\{ t > t_k \mid \tilde{\varepsilon}^T(k) \Omega_1 \tilde{\varepsilon}(k) - \delta_1(k) \rho_y^T(k) \Omega_1 \rho_y(k) > 0 \right\}, g(k) < 0, \\ \text{Conventional ETS : } \min_{k \in \mathbb{N}} \left\{ t > t_k \mid \varepsilon^T(k) \Omega_2 \varepsilon(k) - \delta_2(k) \rho_y^T(k) \Omega_2 \rho_y(k) > 0 \right\}, g(k) \geq 0, \end{cases} \quad (6)$$

where $\rho_y(t_k)$ is the last triggered output, $\tilde{\varepsilon}(k) = \tilde{\rho}_y(k) - \rho_y(t_k)$, $\varepsilon(k) = \rho_y(k) - \rho_y(t_k)$, $\Omega_1 > 0$ and $\Omega_2 > 0$ are the triggering matrices to be designed. Then, for $k \in [t_k, t_{k+1})$, $\delta_1(k)$ and $\delta_2(k)$ are triggering threshold parameters which are determined by the following formula

$$\delta_1(k) = \underline{\delta}_1 + \alpha_1 [\delta_1(k-1) - \underline{\delta}_1 e^{\hat{\delta}_1(k)}], \quad \delta_2(k) = \underline{\delta}_2 + \alpha_2 [\delta_2(k-1) - \underline{\delta}_2 e^{\hat{\delta}_2(k)}], \quad (7)$$

with $0 < \underline{\delta}_1 < \delta_1 < \bar{\delta}_1 = \max \left\{ \delta_1(0), \frac{\underline{\delta}_1}{1-\alpha_1} \right\}$, $0 < \underline{\delta}_2 < \delta_2 < \bar{\delta}_2 = \max \left\{ \delta_2(0), \frac{\underline{\delta}_2}{1-\alpha_2} \right\}$, $0 < \alpha_1 < 1$, $0 < \alpha_2 < 1$, $\hat{\delta}_1(k)$ and $\hat{\delta}_2(k)$ is defined by

$$\hat{\delta}_1(k) = \frac{\tilde{\varepsilon}^T(k) \Omega_1 \tilde{\varepsilon}(k)}{\tilde{\rho}_y^T(k) \Omega_1 \tilde{\rho}_y(k)}, \quad \hat{\delta}_2(k) = \frac{\varepsilon^T(k) \Omega_2 \varepsilon(k)}{\rho_y^T(k) \Omega_2 \rho_y(k)}. \quad (8)$$

Besides, the switching-like function $g(k)$ is designed as follows

$$g(k) = \frac{\left\| \rho_y(t_k) - \rho_y(t_{k-1}) \right\|}{t_k - t_{k-1}} - \beta, \quad (9)$$

where β is a given positive constant. Then, by setting $\mathcal{N}_2 = \{t_0, t_1, t_2, \dots, t_k, \dots\}$, $k \in \mathbb{N}$, which is the set of data packets filtered by (6) that can be transmitted, it is self-evident that $\mathcal{N}_2 \subseteq \mathcal{N}_1$.

Remark 3. As is well known, the conventional ETS can effectively reduce the number of transmitted data, while with less data transmissions, the ETS would cause certain negative impact on control performance. In order to overcome this shortcoming, an event mechanism called memory ETS is proposed to achieve the balance between the reduced data and desirable performance. Yet, the memory ETS is less effective in comparisons with the conventional one. Thus, in this paper, a switching-like ETS is proposed by combining the advantages of the conventional ETS and memory one. Based on such switching-like ETS, the memory ETS is responsible for increasing the probability of triggered at the peak and trough when the composite signal changes slowly, while the conventional one is exploited at the time when the signal changes rapidly to avoid the excessive and unimportant increasing. Obviously, the key of designing the switching-like ETS is how to choose the switching function $g(k)$. By adjusting

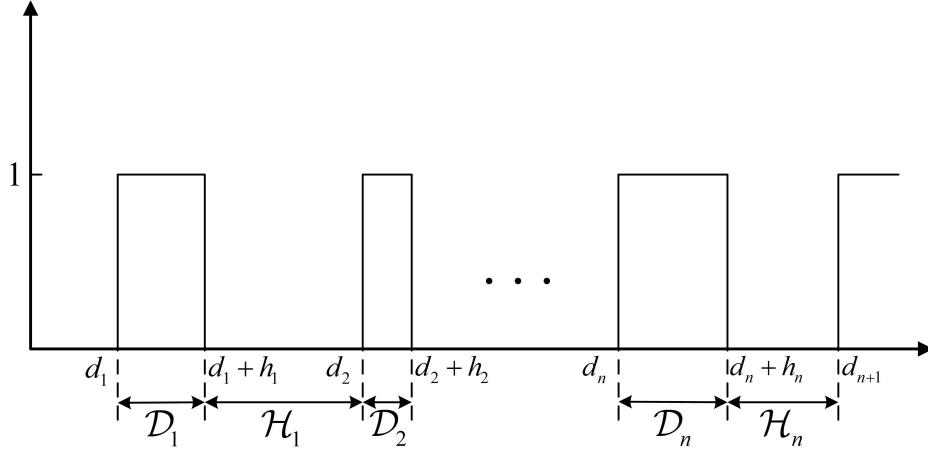


FIGURE 2 The unknown aperiodic DoS attacks signal.

the value β , it is common that $g(k) < 0$ needs to be satisfied at the period of slow change of the composite signal $\varphi_y(k)$, and when the composite signal changes rapidly, $g(k) \geq 0$ holds. It can be checked from (9) that the function $g(k)$ is determined by the previous trigger instant $\varphi_y(t_k - 1)$ and the current one $\varphi_y(t_k)$, which decides to switch the suitable ETS and reflects the change rate of $\varphi_y(k)$.

As shown in Fig. 1, the DoS attacks will prevent the update of data transmissions during the tracking procedure, that is to say, the data packets triggered by switching-like ETS will be lost, which can be modeled as a piecewise function. By referring to³⁹, the occurrence periods of DoS attacks can be shown in Fig. 2 and further described as follows

$$D(k) = \begin{cases} 1, & k \in D_n, \\ 0, & k \in H_n, \end{cases} \quad (10)$$

where the intervals $D_n = [d_n, d_n + h_n)$ and $H_n = [d_n + h_n, d_{n+1})$ denote the active interval of the n th DoS attacks and the sleep one of the n th DoS attacks, respectively, $n \in \mathbb{N}_{\geq 0}$. It is worth noting that $h_n \in \mathbb{N}$ represents the duration of the DoS attacks and $d_n \in \mathbb{N}$. In addition, when $h_n = 0$, it indicates that a single pulse DoS attack is generated at time d_n . Therefore, all attack intervals make up the period of the whole DoS attack

$$\mathcal{I}_{DoS}(k) = \bigcup_{n \in \mathbb{N}_{\geq 0}} D_n. \quad (11)$$

The difference from²⁹ is that the duration and frequency of the DoS attacks are not limited, while there exist agreements on its energy based on the following assumption.

Assumption 3.³¹ The maximum number of packets losses induced by the DoS attacks is not greater than M , and $M \in \mathbb{N}$.

By setting $\mathcal{N}_3 = \{s_0, s_1, s_2, \dots, s_k, \dots\}$, $k \in \mathbb{N}$, it denotes the triggered sequence of the successful transmission under the DoS attacks. It can be checked that $\mathcal{N}_3 \subseteq \mathcal{N}_2 \subseteq \mathcal{N}_1$. In order to clearly describe our switching-like ETS, the following lemma is introduced to classify the transmission behaviors for successful triggering instances.

Lemma 1.³¹ There exist two situations between the moments of successful triggered intervals $[s_k, s_{k+1})$, $k \in \mathbb{N}$. That is, one is S-interval \mathcal{I} without DoS attack, and the other is A-interval $\tilde{\mathcal{I}}$ under DoS attacks

(1) S-interval \mathcal{I} : If $[s_k, s_{k+1}) \cap \mathcal{I}_{DoS}(k) = \emptyset$, $ACK = 1$,

(2) A-interval $\tilde{\mathcal{I}}$: If $[s_k, s_{k+1}) \cap \mathcal{I}_{DoS}(k) \neq \emptyset$, $ACK = 0$.

Based on above discussions, a new ETS is introduced to deal with this problem

$$s_{k+1} = \min_{k \in \mathbb{N}} \left\{ t > s_k \mid \varepsilon^T(k) \Omega_3 \varepsilon(k) - \delta_3 \varphi_y^T(k) \Omega_3 \varphi_y(k) > 0 \right\}, \quad (12)$$

where $\varepsilon(k) = \varphi_y(k) - \varphi_y(s_k)$, Ω_3 is the triggering matrix to be designed, and $\delta_3 > 0$ denotes the preset triggering threshold.

Remark 4. As described in Fig. 3, the concept of the ACK is presented and it is used to detect whether DoS attacks exist at the instants of triggered transmission. If $ACK = 1$, it means $k \in \mathcal{I}$ and the current triggered instant without the DoS attacks,

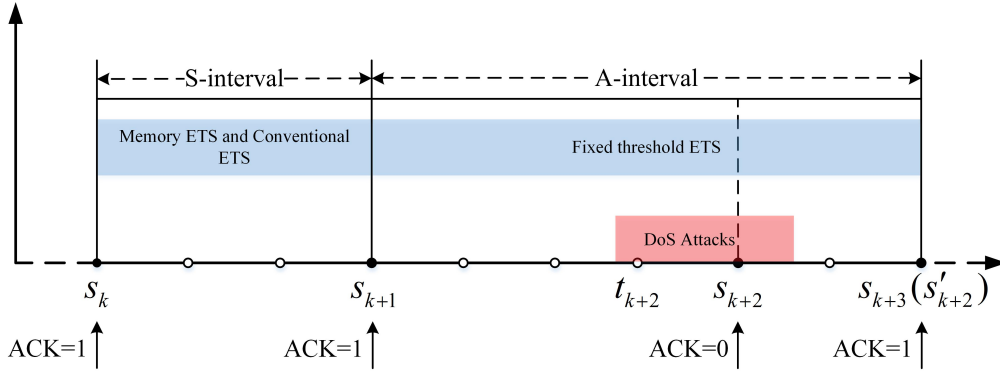


FIGURE 3 The structure of switching-like of ETS under DoS attacks.

then (6) is used to trigger according to function $g(k)$, otherwise, (12) is triggered and $ACK = 0$, $k \in \tilde{\mathcal{I}}$. It is worth noting that during the transmission to ETS, the ACK signal may also be lost due to DoS attacks, which is classified as $ACK = 0$.

To sum up, the switching-like ETS under DoS attacks can be described as follows

$$s_{k+1} = \begin{cases} \text{Memory ETS : } \min_{k \in \mathbb{N}} \left\{ t > s_k | \tilde{\varepsilon}^T(k) \Omega_1 \tilde{\varepsilon}(k) - \delta_1(k) \rho_y^T(k) \Omega_1 \rho_y(k) > 0 \right\}, g(k) < 0, ACK = 1, \\ \text{Conventional ETS : } \min_{k \in \mathbb{N}} \left\{ t > s_k | \varepsilon^T(k) \Omega_2 \varepsilon(k) - \delta_2(k) \rho_y^T(k) \Omega_2 \rho_y(k) > 0 \right\}, g(k) \geq 0, ACK = 1, \\ \text{Fixed threshold ETS : } \min_{k \in \mathbb{N}} \left\{ t > s_k | \varepsilon^T(k) \Omega_3 \varepsilon(k) - \delta_3 \rho_y^T(k) \Omega_3 \rho_y(k) > 0 \right\}, ACK = 0, \end{cases} \quad (13)$$

where $\tilde{\varepsilon}(k) = \tilde{\rho}_y(k) - \rho(s_k) = [\tilde{\varepsilon}_{y_i}^T(k), \tilde{\varepsilon}_r^T(k)]^T$, $\varepsilon(k) = \rho_y(k) - \rho(s_k) = [\varepsilon_{y_a}^T(k), \varepsilon_r^T(k)]^T$. Then, the data triggered by the ETS in (13) can be admitted for transmission via communication network, which are utilized to design the observer to estimate the UGV state and the reference signal.

2.3 | Estimations of the states, disturbance, and reference signal

For the UGV, since the observer is installed in the UAH, it is necessary to use the triggered data to estimate its state $\hat{x}_a(k)$ and reference $r(k)$, as shown below

$$\begin{cases} \hat{x}_a(k+1) = (A_a + B_a K_a C_a) \hat{x}_a(k) + B_r \hat{r}(k) + L_1(k) [y_a(s_k) - \tilde{y}_a(k)], \\ \hat{r}(k+1) = \hat{r}(k) + L_2(k) [r(s_k) - \tilde{r}(k)], \\ \hat{y}_a(k) = C_a \hat{x}_a(k), \end{cases} \quad (14)$$

where $\hat{x}_a(k) \in \mathbb{R}^{2 \times 1}$ represents the observation state of UGV, $\tilde{y}_a \in \mathbb{R}^{2 \times 1}$ means the observation output of UGV, $\tilde{r}(k) \in \mathbb{R}^{2 \times 1}$ indicates the estimation of reference signal $r(k)$. Moreover, $L_1(k), L_2(k) \in \mathbb{R}^{2 \times 2}$ are the observer gains and designed as follows

$$L_1(k) = \begin{cases} L_{11}, & k \in \mathcal{D}_n, \\ L_{12}, & k \in \mathcal{H}_n, \end{cases} \quad L_2(k) = \begin{cases} L_{21}, & k \in \mathcal{D}_n, \\ L_{22}, & k \in \mathcal{H}_n. \end{cases} \quad (15)$$

For the UAH system, since the signals of its state and observer are not affected by the DoS attacks, then its state observer and disturbance one are designed as follows

$$\begin{cases} \hat{x}_b(k+1) = A_b \hat{x}_b(k) + B_b u_b(k) + B_d \hat{d}(k) + L_3 [y_b(k) - \hat{y}_b(k)], \\ \hat{d}(k+1) = \hat{d}(k) + L_4 [y_b(k) - \hat{y}_b(k)], \\ \hat{y}_b(k) = C_b \hat{x}_b(k), \end{cases} \quad (16)$$

where $\hat{x}_b(k) \in \mathbb{R}^{4 \times 1}$ means the observation state of UAH system, $\hat{y}_b(k) \in \mathbb{R}^{2 \times 1}$ represents the observation output of UAH system, $\hat{d}(k) \in \mathbb{R}^{2 \times 1}$ expresses the estimation of disturbance $d(k)$, $L_3 \in \mathbb{R}^{4 \times 2}$, $L_4 \in \mathbb{R}^{2 \times w}$ are the observer gains.

Define the estimation errors as $e_{x_a}(k) = x_a(k) - \hat{x}_a(k)$, $e_{x_b}(k) = x_b(k) - \hat{x}_b(k)$, $e_r(k) = r(k) - \hat{r}(k)$, and $e_d(k) = d(k) - \hat{d}(k)$. In addition, $\tilde{e}_{x_a}(k) = \sum_{i=0}^{m-1} p_i e_{x_a}(k-i)$ and $\tilde{e}_r(k) = \sum_{i=0}^{m-1} p_i e_r(k-i)$. By combining (1), (2), (14), (15), and (16), the closed-loop system on estimation errors can be summarized in the following cases

- (1) When the DoS attacks does not occur, $ACK = 1$,
 (i) $g(k) < 0$,

$$\begin{cases} e_{x_a}(k+1) = (A_a + B_a K_a C_a) e_{x_a}(k) + B_r e_r(k) - L_{12} C_a \tilde{e}_{x_a}(k) + L_{12} \tilde{e}_{y_a}(k), \\ e_r(k+1) = e_r(k) - L_{22} \tilde{e}_r(k) + L_{22} \tilde{e}_r(k) + \Delta r(k), \\ e_{x_b}(k+1) = (A_b - L_3 C_b) e_{x_b}(k) + B_d e_d(k), \\ e_d(k+1) = e_d(k) - L_4 C_b e_{x_b}(k) + \Delta d(k). \end{cases} \quad (17)$$

- (ii) $g(k) \geq 0$, at this time, $\tilde{y}_a(k) = \hat{y}_a(k)$, $\tilde{r}(k) = \hat{r}(k)$,

$$\begin{cases} e_{x_a}(k+1) = (A_a + B_a K_a C_a - L_{12} C_a) e_{x_a}(k) + B_r e_r(k) + L_{12} \varepsilon_{y_a}(k), \\ e_r(k+1) = (I_2 - L_{22}) e_r(k) + L_{22} \varepsilon_r(k) + \Delta r(k), \\ e_{x_b}(k+1) = (A_b - L_3 C_b) e_{x_b}(k) + B_d e_d(k), \\ e_d(k+1) = e_d(k) - L_4 C_b e_{x_b}(k) + \Delta d(k). \end{cases} \quad (18)$$

- (2) When the DoS attacks occur, $ACK = 0$,

$$\begin{cases} e_{x_a}(k+1) = (A_a + B_a K_a C_a) e_{x_a}(k) + B_r e_r(k) - L_{11} C_a e_{x_a}(k) + L_{11} \varepsilon_{y_a}(k), \\ e_r(k+1) = (I_2 - L_{21}) e_r(k) + L_{21} \varepsilon_r(k) + \Delta r(k), \\ e_{x_b}(k+1) = (A_b - L_3 C_b) e_{x_b}(k) + B_d e_d(k), \\ e_d(k+1) = e_d(k) - L_4 C_b e_{x_b}(k) + \Delta d(k). \end{cases} \quad (19)$$

2.4 | Design of anti-disturbance tracking controller

The goal of this paper is to design the tracking control scheme of the UAH/UGV systems based on the switching-like ETS against DoS attacks and external disturbance, which means that the difference between the output of the UAH and the UGV needs to be bounded, such as $y_b(k) - y_a(k)$. Because of the different dimensions between them, by assuming $C_b = C_a S_b$, if $S_b x_b(k) - x_a(k)$ is bounded, it can be ensured that $y_b(k) - y_a(k)$ is also bounded. In this way, by defining the tracking error between the UAH and UGV as $e(k) = S_b x_b(k) - x_a(k)$, one can derive

$$e(k+1) = S_b A_b x_b(k) + S_b B_b u_b(k) + S_b B_d d(k) - (A_a + B_a K_a C_a) x_a(k) - B_r r(k). \quad (20)$$

Once again, its observation value $\hat{e}(k) = S_b \hat{x}_b(k) - \hat{x}_a(k)$ can be got by the observations $\hat{x}_a(k)$ and $\hat{x}_b(k)$. Then, it follows from (14), (15) and (16) that the tracking controller is designed as follows

$$u_b(k) = \begin{cases} K_1 \hat{e}(k) + K_b \hat{x}_b(k) + K_r \hat{r}(k) - K_d \hat{d}(k), & ACK = 1, \\ K_2 \hat{e}(k) + K_b \hat{x}_b(k) + K_r \hat{r}(k) - K_d \hat{d}(k), & ACK = 0. \end{cases} \quad (21)$$

Now, by taking the case $ACK = 1$ as an example, the first line of (21) is brought into (20)

$$\begin{aligned} e(k+1) &= (S_b A_b + S_b B_b K_b) x_b(k) - (A_a + B_a K_a C_a) x_a(k) + S_b B_b K_1 e(k) + S_b B_b K_1 e_a(k) - S_b B_r K_r e_r(k) \\ &\quad + S_b B_b K_r r(k) - B_r r(k) - S_b B_b K_d \hat{d}(k) - S_b B_b K_b e_b(k) - S_b B_b K_1 S_b e_b(k) + S_b B_d d(k). \end{aligned} \quad (22)$$

By denoting the vectors $e_{ar}(k) = [e_{x_a}^T(k), e_r^T(k)]^T$, $\tilde{e}_{ar}(k) = [\tilde{e}_{x_a}^T(k), \tilde{e}_r^T(k)]^T$, $e_{bd}(k) = [e_{x_b}^T(k), e_d^T(k)]^T$, and according to Assumption 2, there must exist matrices K_b , K_r , and K_d such that $S_b A_b + S_b B_b K_b = (A_a + B_a K_a C_a) S_b$, $S_b B_b K_r = B_r$, and $B_b K_d = B_d$. Then the tracking error (20) can be rewritten as

$$e(k+1) = \begin{cases} (\bar{A}_a + \bar{B}_b K_1) e(k) + (\bar{B}_b K_1 E_3 - \bar{B}_b K_r E_1^T) e_{ar}(k) + (\bar{B}_b K_d E_2^T - \bar{B}_b K_b E_4 - \bar{B}_b K_1 S_b E_4) e_{bd}(k), & ACK = 1, \\ (\bar{A}_a + \bar{B}_b K_2) e(k) + (\bar{B}_b K_2 E_3 - \bar{B}_b K_r E_1^T) e_{ar}(k) + (\bar{B}_b K_d E_2^T - \bar{B}_b K_b E_4 - \bar{B}_b K_2 S_b E_4) e_{bd}(k), & ACK = 0, \end{cases} \quad (23)$$

where $\bar{A}_a = A_a + B_a K_a C_a$, $\bar{B}_b = S_b B_b$, $E_1 = [0, I_2]_{4 \times 2}^T$, $E_2 = [0, I_2]_{(4+u) \times w}^T$, $E_3 = [I_2, 0]_{2 \times 4}$, and $E_4 = [I_4, 0]_{4 \times (4+u)}$.

Then, after the error dynamics of the UAH/UGV systems are analyzed synthetically, the augmented closed-loop systems (17), (18), (19) and (23) in three cases are summarized in what follows

(1) $ACK = 1$,

(i) $g(k) < 0$,

$$\begin{cases} e_{ar}(k+1) = A_{ar}e_{ar}(k) - L_{ar}C_{ar}\tilde{e}_{ar}(k) + L_{ar}\tilde{\varepsilon}(k) + E_1\Delta r(k), \\ e_{bd}(k+1) = (A_{bd} - L_{bd}C_{bd})e_{bd}(k) + E_2\Delta d(k), \\ e(k+1) = (\bar{A}_a + \bar{B}_bK_1)e(k) + (\bar{B}_bK_1E_3 - \bar{B}_bK_rE_1^T)e_{ar}(k) + (\bar{B}_bK_dE_2^T - \bar{B}_bK_bE_4 - \bar{B}_bK_1S_bE_4)e_{bd}(k). \end{cases} \quad (24)$$

(ii) $g(k) \geq 0$,

$$\begin{cases} e_{ar}(k+1) = (A_{ar} - L_{ar}C_{ar})e_{ar}(k) + L_{ar}\varepsilon(k) + E_1\Delta r(k), \\ e_{bd}(k+1) = (A_{bd} - L_{bd}C_{bd})e_{bd}(k) + E_2\Delta d(k), \\ e(k+1) = (\bar{A}_a + \bar{B}_bK_1)e(k) + (\bar{B}_bK_1E_3 - \bar{B}_bK_rE_1^T)e_{ar}(k) + (\bar{B}_bK_dE_2^T - \bar{B}_bK_bE_4 - \bar{B}_bK_1S_bE_4)e_{bd}(k). \end{cases} \quad (25)$$

(2) $ACK = 0$,

$$\begin{cases} e_{ar}(k+1) = (A_{ar} - \bar{L}_{ar}C_{ar})e_{ar}(k) + \bar{L}_{ar}\varepsilon(k) + E_1\Delta r(k), \\ e_{bd}(k+1) = (A_{bd} - L_{bd}C_{bd})e_{bd}(k) + E_2\Delta d(k), \\ e(k+1) = (\bar{A}_a + \bar{B}_bK_2)e(k) + (\bar{B}_bK_2E_3 - \bar{B}_bK_rE_1^T)e_{ar}(k) + (\bar{B}_bK_dE_2^T - \bar{B}_bK_bE_4 - \bar{B}_bK_2S_bE_4)e_{bd}(k), \end{cases} \quad (26)$$

where

$$\begin{aligned} A_{ar} &= \begin{bmatrix} \bar{A}_a & B_r \\ 0 & I_2 \end{bmatrix}, \quad A_{bd} = \begin{bmatrix} A_b & B_d \\ 0 & I_w \end{bmatrix}, \quad C_{ar} = \begin{bmatrix} C_a & 0 \\ 0 & I_2 \end{bmatrix}, \quad C_{bd} = [C_b \ 0], \quad L_{ar} = \begin{bmatrix} L_{12} & 0 \\ 0 & L_{22} \end{bmatrix}, \\ \bar{L}_{ar} &= \begin{bmatrix} L_{11} & 0 \\ 0 & L_{21} \end{bmatrix}, \quad L_{bd} = \begin{bmatrix} L_3 \\ L_4 \end{bmatrix}. \end{aligned}$$

Remark 5. Compared with the Ref. ¹⁴, the trajectory tracking control method proposed in this paper utilizes the ACK technology to nest a new handover scheme on the periphery of the switching-like ETS for handling the DoS attacks. Moreover, together with the switching-like ETS, the observers and the controller with switch gains are presented on the basis of the properties of DoS attacks. These strategies can not only achieve better balance between data transmission volume and control performance, but also weaken the negative impact caused by the disturbance and DoS attacks.

To get a further deduction, two augmented vectors $\varphi_1(k)$, $\varphi_2(k)$ are defined as follows

$$\begin{aligned} \varphi_1(k) &= [\rho^T(k), e_{ar}^T(k), e_{ar}^T(k-1), \dots, e_{ar}^T(k+1-m), e_{bd}^T(k), e^T(k), \tilde{\varepsilon}^T(k), \Delta r^T(k), \Delta d^T(k)]^T, \\ \varphi_2(k) &= [\rho^T(k), e_{ar}^T(k), e_{bd}^T(k), e^T(k), \varepsilon^T(k), \Delta r^T(k), \Delta d^T(k)]^T, \end{aligned}$$

with $\rho(k) = [x_a^T(k), r^T(k)]^T$.

In order to analyze the stability of the augmented closed-loop system and complete the controller design, the following definition and lemmas are introduced.

Definition 1.³⁷ For a disturbed system, it is described as a discrete-time form $x(k+1) = f(k, x(k), d(k))$, if there exist the scalars $\lambda \geq 0$, $\mu > 0$, $v > 0$ such that a Lyapunov function $V(x(k))$ meets

$$\mu \|x(k)\|^2 \leq V(x(k)) \leq v \|x(k)\|^2,$$

and

$$V(x(k+1)) - V(x(k)) \leq \lambda - \tau V(x(k)),$$

then the solutions of the system are uniformly ultimately bounded with the upper bound $\sqrt{\frac{\lambda+\varepsilon}{\mu}}$, where $\varepsilon > 0$ is an arbitrarily small scalar.

Lemma 2.⁴⁰ The conditions in (a) and (b) are equivalent when two following inequalities are satisfied

(a) There exists a symmetric matrix $P > 0$ satisfying

$$\begin{bmatrix} -P & A^T \\ A & -P^{-1} \end{bmatrix} < 0.$$

(b) There exist two matrices $P > 0$ and Y satisfying

$$\begin{bmatrix} -P & (YA)^T \\ YA & \text{He}(-Y) + P \end{bmatrix} < 0.$$

Lemma 3.¹⁸ Given the suitable matrices O , $P(k)$, and Q with $P(k)$ satisfying $P^T(k)P(k) \leq I$, for any scalar $\sigma > 0$, the following inequality holds

$$OP(k)Q + Q^T P^T(k)O^T \leq \sigma OO^T + \sigma^{-1} Q^T Q.$$

3 | MAIN RESULTS

In this section, as for the switching-like ETS (13), the relationships between the maximum number of packets losses M under the DoS attacks and $\bar{\delta}_1$, $\bar{\delta}_2$, δ_3 are first given in Theorem 1. Then, as for the ETS in (13), the gain-switchable observers (14), (16) and the gain-switchable tracking controller (21), a co-design scheme of switching-like ETS is proposed, and the uniform ultimate boundedness of the system (24)-(26) is performed in Theorem 2. Finally, by solving the nonlinear terms in Theorem 2, in Theorem 3, a co-design method of checking the triggering parameters, observer gains, and controller gains is established in terms of the LMIs, which can be easily tested by resorting to the Matlab LMI Toolbox.

Theorem 1. Given the UAH system (1) and UGV system (2), the scalar M in Assumption 3 and a positive constrained constant η , the DoS attacks can be resolved if $\bar{\delta}_1$, $\bar{\delta}_2$, and δ_3 satisfy

$$\sqrt{\delta_3} + 2(\sqrt{\delta_3})^M + \xi^M(1 + \sqrt{\delta_3})^M \leq \sqrt{\delta_2}, \quad \sqrt{\delta_3} + 2(\sqrt{\delta_3})^M + \xi^M(1 + \sqrt{\delta_3})^M \leq \frac{1}{p_0} \sqrt{\bar{\delta}_1}, \quad (27)$$

where $\xi_1 = \|(A_a - I_2)h\| + \left\| \frac{hB_a K_a C_a}{1 - \sqrt{\delta_1}} \right\| + \|\eta h B_r\|$ and $\xi_2 = \|(A_a - I_2)h\| + \left\| \frac{hB_a K_a C_a}{1 - \sqrt{\delta_2}} \right\| + \|\eta h B_r\|$.

Proof. When the DoS attacks occur, suppose that there are successive M packet losses with $s_k = l_0 < l_1 < l_2 < \dots < l_j < \dots < l_M < l_{M+1} = s_{k+1}$ under the trigger instances of the third line in (13). Applying the third event-triggered condition yields $\|\varrho_y(k) - \varrho_y(l_j)\| \leq \sqrt{\delta_3} \|\varrho_y(k)\|$, such that

$$\|x_a(l_{j+1} - h) - x_a(k)\| \leq \sqrt{\delta_3} \|x_a(k)\|. \quad (28)$$

In what follows, a new inequality is introduced as

$$\|x_a(l_{j+1} - h)\| \leq \|x_a(l_{j+1} - h) - x_a(k)\| + \|x_a(k)\| \leq \sqrt{\delta_3} \|x_a(k)\| + \|x_a(k)\| \leq (1 + \sqrt{\delta_3}) \|x_a(k)\|. \quad (29)$$

Then, according to the second line of (13), $\|x_a(k)\|$ is magnified to

$$\|x_a(k)\| \leq \|x_a(l_{j+1} - h)\| + \|x_a(l_{j+1} - h) - x_a(k)\| \leq \|x_a(l_{j+1} - h)\| + \sqrt{\delta_2} \|x_a(k)\|. \quad (30)$$

As for the reference signal $r(k)$, according to Assumption 1 and the solution of $x(k)|_{k=l_{j+1}}$ of (13) and (30), it has

$$\begin{aligned} \|x_a(l_{j+1}) - x_a(l_{j+1} - h)\| &= \|(A_a - I_2)x_a(l_{j+1} - h) + B_a K_a C_a x_a(k) + B_r r(l_{j+1} - h)\| \\ &\leq \|(A_a - I_2)h x_a(l_{j+1} - h)\| + \|B_a h K_a C_a x_a(k)\| + \|B_r h r(l_{j+1} - h)\| \\ &\leq \xi_2 \|x_a(l_{j+1} - h)\|. \end{aligned} \quad (31)$$

Next, by combining (29) and (31), it can be derived as

$$\|x_a(l_{j+1}) - x_a(l_{j+1} - h)\| \leq \xi_2 (1 + \sqrt{\delta_3}) \|x_a(k)\|. \quad (32)$$

For $k \in [l_M, l_{M+1})$, the state error between the seconds k and s_k is

$$\begin{aligned} \|x_a(k) - x_a(s_k)\| &= \|x_a(k) - x_a(l_0)\| \\ &\leq \|x_a(k) - x_a(l_M)\| + \sum_{j=0}^{M-1} \|x_a(l_{j+1} - h) - x_a(l_j)\| + \sum_{j=0}^{M-1} \|x_a(l_{j+1}) - x_a(l_{j+1} - h)\|. \end{aligned} \quad (33)$$

Among (33), the second term satisfies

$$\sum_{j=0}^{M-1} \|x_a(l_{j+1} - h) - x_a(l_j)\| \leq \sum_{j=0}^{M-1} \|x_a(k) - x_a(l_{j+1} - h)\| + \sum_{j=0}^{M-1} \|x_a(k) - x_a(l_j)\| \leq 2 \sum_{j=0}^{M-1} \sqrt{\delta_3} \|x_a(k)\|, \quad (34)$$

and from (28),(32) and (34), one can obtain that

$$\begin{aligned} \|x_a(k) - x_a(s_k)\| &\leq \sqrt{\delta_3} \|x_a(k)\| + 2 \sum_{j=0}^{M-1} \sqrt{\delta_3} \|x_a(k)\| + \sum_{j=0}^{M-1} \xi(1 + \sqrt{\delta_3}) \|x_a(k)\| \\ &\leq \left[2(\sqrt{\delta_3})^M + \sqrt{\delta_3} + \xi_2^M(1 + \sqrt{\delta_3})^M \right] \|x_a(k)\|. \end{aligned} \quad (35)$$

By considering (13), when no DoS attacks occur and $g(k) > 0$, such that $\|x_a(k) - x_a(s_k)\| \leq \sqrt{\delta_2} \|x_a(k)\|$, the relationship between $\bar{\delta}_2$ and δ_3 is

$$\sqrt{\delta_3} + 2(\sqrt{\delta_3})^M + \xi_2^M(1 + \sqrt{\delta_3})^M \leq \sqrt{\delta_2}. \quad (36)$$

On the other hand, as for $g(k) < 0$, the proof process is similar to the above, and the relationship between $\bar{\delta}_1$ and δ_3 yields

$$\sqrt{\delta_3} + 2(\sqrt{\delta_3})^M + \xi_1^M(1 + \sqrt{\delta_3})^M \leq \frac{1}{p_0} \sqrt{\delta_1}. \quad (37)$$

The proof is completed.

In what follows, based on Theorem 1, a stability criterion is established to ensure the bounded stability for the systems (24)-(26), which can be checked in the follow theorem.

Theorem 2. For some given positive constants $o_1, o_2, o_3, o_4, o_5, \bar{\delta}_1, \bar{\delta}_2, \delta_3, p_i$ ($i = 0, \dots, m-1$) and matrices S_b, K_a, K_b, K_r, K_d are obtained by (3) and Assumption 2, under the switching-like ETS scheme(13), the gain-switchable observer (14), (16), and the gain-switchable tracking controller (21), the augmented closed-loop error system (24)-(26) is uniformly ultimately bounded if there exist suitable matrices $P_1 > 0, P_2 > 0, P_3 > 0, P_4 > 0, \Omega_1 > 0, \Omega_2 > 0, \Omega_3 > 0$ such that

$$\Gamma_1 = \begin{bmatrix} \Gamma_1^{11} & \Gamma_1^{12} \\ * & \Gamma_1^{22} \end{bmatrix} < 0, \Gamma_2 = \begin{bmatrix} \Gamma_2^{11} & \Gamma_2^{12} \\ * & \Gamma_2^{22} \end{bmatrix} < 0, \Gamma_3 = \begin{bmatrix} \Gamma_3^{11} & \Gamma_3^{12} \\ * & \Gamma_3^{22} \end{bmatrix} < 0, \quad (38)$$

where

$$\begin{aligned} \Gamma_1^{11} &= \Phi_1, \Gamma_2^{11} = \Phi_2, \Gamma_3^{11} = \Phi_3, \Gamma_1^{12} = [T_1^T, T_2^T, T_3^T, T_4^T], \Gamma_2^{12} = [T_5^T, T_6^T, T_7^T, T_8^T], \\ \Gamma_3^{12} &= [T_9^T, T_{10}^T, T_{11}^T, T_{12}^T], \Gamma_1^{22} = \Gamma_2^{22} = \Gamma_3^{22} = \text{diag}(-P_1, -P_2, -P_3, -P_4), \end{aligned}$$

with

$$\begin{aligned} \Phi_1 &= [\Phi_1^{ij}]_{7 \times 7}, \Phi_2 = [\Phi_2^{ij}]_{7 \times 7}, \Phi_3 = [\Phi_3^{ij}]_{7 \times 7}, \\ \Phi_1^{11} &= \bar{\delta}_1 C_{ar}^T \Omega_1 C_{ar} - E_3^T P_1 E_3 - E_1 I_2 E_1^T, \Phi_2^{11} = \bar{\delta}_2 C_{ar}^T \Omega_2 C_{ar} - E_3^T P_1 E_3 - E_1 I_2 E_1^T, \\ \Phi_3^{11} &= \delta_3 C_{ar}^T \Omega_3 C_{ar} - E_3^T P_1 E_3 - E_1 I_2 E_1^T, \Phi_1^{22} = \text{diag}[(p_1^2 - p_0^2) P_2, (p_2^2 - p_1^2) P_2, \dots, (-p_{m-1}^2) P_2], \\ \Phi_2^{22} &= \Phi_3^{22} = -P_2, \Phi_1^{33} = \Phi_2^{33} = \Phi_3^{33} = -P_3, \Phi_1^{44} = \Phi_2^{44} = \Phi_3^{44} = -P_4, \Phi_1^{55} = -\Omega_1, \\ \Phi_2^{55} &= -\Omega_2, \Phi_3^{55} = -\Omega_3, \Phi_1^{66} = \Phi_2^{66} = \Phi_3^{66} = -I_2, \Phi_1^{77} = \Phi_2^{77} = \Phi_3^{77} = -I_w, \\ T_1 &= [P_1 E_3 A_{ar}, \underbrace{0, 0, \dots, 0}_{m-1}, 0, 0, 0, 0, 0], \\ T_2 &= [0, p_0^2 P_2 A_{ar} - p_0^2 P_2 L_{ar} C_{ar}, -p_0^2 p_1 P_2 L_{ar} C_{ar}, \dots, -p_0^2 p_{m-1} P_2 L_{ar} C_{ar}, 0, 0, P_2 L_{ar}, P_2 E_1, 0], \\ T_3 &= [0, 0, 0, \dots, 0, \underbrace{P_3 A_{bd} - P_3 L_{bd} C_{bd}}_{m-1}, 0, 0, 0, P_3 E_2], T_4 = [0, T_4^1, 0, \dots, 0, \underbrace{T_4^2, T_4^3}_{m-1}, 0, 0, 0], \\ T_4^1 &= P_4 \bar{B}_b K_1 E_3 - P_4 \bar{B}_b K_r E_1^T, T_4^2 = P_4 \bar{B}_b K_d E_2^T - P_4 \bar{B}_b K_b E_4 - P_4 \bar{B}_b K_1 S_b E_4, T_4^3 = P_4 \bar{A}_a + P_4 \bar{B}_b K_1, \\ T_5 &= [P_1 E_3 A_{ar}, 0, 0, 0, 0, 0, 0], T_6 = [0, P_2 A_{ar} - P_2 L_{ar} C_{ar}, 0, 0, P_2 L_{ar}, P_2 E_1, 0], \\ T_7 &= [0, 0, P_3 A_{bd} - P_3 L_{bd} C_{bd}, 0, 0, 0, P_3 E_2, 0], T_8 = [0, T_8^1, T_8^2, T_8^3, 0, 0, 0], T_8^1 = T_4^1, T_8^2 = T_4^2, \\ T_8^3 &= T_4^3, T_9 = T_5, T_{10} = [0, P_2 A_{ar} - P_2 \bar{L}_{ar} C_{ar}, 0, 0, P_2 \bar{L}_{ar}, P_2 E_1, 0], T_{11} = T_7, \\ T_{12} &= [0, T_{12}^1, T_{12}^2, T_{12}^3, 0, 0, 0], T_{12}^1 = P_4 \bar{B}_b K_2 E_3 - P_4 \bar{B}_b K_r E_1^T, \\ T_{12}^2 &= P_4 \bar{B}_b K_d E_2^T - P_4 \bar{B}_b K_b E_4 - P_4 \bar{B}_b K_2 S_b E_4, T_{12}^3 = P_4 \bar{A}_a + P_4 \bar{B}_b K_2. \end{aligned}$$

Proof. For $k \in [s_k, s_{k+1})$, a Lyapunov function $V(k)$ is constructed as follows

$$V(k) = x_a^T(k) P_1 x_a(k) + \tilde{e}_{ar}^T(k) P_2 \tilde{e}_{ar}(k) + e_{bd}^T(k) P_3 e_{bd}(k) + e^T(k) P_4 e(k), \quad (39)$$

and $V(k)$ satisfies $\lambda_1 \|\varphi_2(k)\|^2 \leq V(k) \leq \lambda_2 \|\varphi_2(k)\|^2$ with two positive scalars λ_1 and λ_2 .

Initially, from Assumption 1, one can obtain that

$$r^T(k)r(k) \leq o_1^2, \Delta r^T(k)\Delta r(k) \leq o_3^2, \Delta d^T(k)\Delta d(k) \leq o_4^2. \quad (40)$$

By using the switching-like ETS (13) and for $k \in [s_k, s_{k+1})$, the following inequalities can be obtained as

$$\begin{cases} \tilde{\varepsilon}^T(k)\Omega_1\tilde{\varepsilon}(k) - \bar{\delta}_1\phi_y^T(k)\Omega_1\phi_y(k) \leq 0, g(k) < 0, ACK = 1, \\ \varepsilon^T(k)\Omega_2\varepsilon(k) - \bar{\delta}_2\phi_y^T(k)\Omega_2\phi_y(k) \leq 0, g(k) \geq 0, ACK = 1, \\ \varepsilon^T(k)\Omega_3\varepsilon(k) - \bar{\delta}_3\phi_y^T(k)\Omega_3\phi_y(k) \leq 0, ACK = 0. \end{cases} \quad (41)$$

The specific description of the differences of $V(k)$ yields

$$\begin{aligned} \Delta V(k) &= \phi^T(k+1)E_3^T P_1 E_3 \phi(k+1) + \tilde{e}_{ar}^T(k+1)P_2 \tilde{e}_{ar}(k+1) + e_{bd}^T(k+1)P_3 e_{bd}(k+1) \\ &\quad + e^T(k+1)P_4 e(k+1) - \phi^T(k)E_3^T P_1 E_3 \phi(k) - \tilde{e}_{ar}^T(k)P_2 \tilde{e}_{ar}(k) - e_{bd}^T(k)P_3 e_{bd}(k) \\ &\quad + e^T(k)P_4 e(k) - r^T(k)r(k) + r^T(k)r(k). \end{aligned} \quad (42)$$

Now, by using the systems in (24)-(26) and (40)-(41), the difference of $\Delta V(k)$ needs to be estimated in three following cases

Case I: As for $ACK = 1, g(k) < 0$, and it follows from (24), (40) and (41) that (42) is amplified to

$$\begin{aligned} \Delta V(k) &\leq \bar{\delta}_1 \phi^T(k) C_{ar}^T \Omega_1 C_{ar} \phi(k) - \phi^T(k) E_3^T P_1 E_3 \phi(k) - r^T(k)r(k) + \{ [p_0 e_{ar}(k+1) + p_1 e_{ar}(k) \\ &\quad + \dots + p_{m-1} e_{ar}(k+2-m)]^T P_2 [p_0 e_{ar}(k+1) + p_1 e_{ar}(k) + \dots + p_{m-1} e_{ar}(k+2-m)] \\ &\quad - [p_0 e_{ar}(k) + p_1 e_{ar}(k-1) + \dots + p_{m-1} e_{ar}(k+1-m)]^T P_2 [p_0 e_{ar}(k) + p_1 e_{ar}(k-1) \\ &\quad + \dots + p_{m-1} e_{ar}(k+1-m)] \} - e_{bd}^T(k)P_3 e_{bd}(k) - e^T(k)P_4 e(k) - \tilde{\varepsilon}^T(k)\Omega_1\tilde{\varepsilon}(k) \\ &\quad - \Delta r^T(k)\Delta r(k) - \Delta d^T(k)\Delta d(k) + \phi^T(k+1)E_3^T P_1 E_3 \phi(k+1) + e_{bd}^T(k+1)P_3 e_{bd}(k+1) \\ &\quad + e^T(k+1)P_4 e(k+1) + r^T(k)r(k) + \Delta r^T(k)\Delta r(k) + \Delta d^T(k)\Delta d(k) \\ &= \phi_1(k)^T(k)\Phi_1\phi_1(k) + \phi^T(k+1)E_3^T P_1 E_3 \phi(k+1) + p_0^2 e_{ar}^T(k+1)P_2 e_{ar}(k+1) \\ &\quad + e_{bd}^T(k+1)P_3 e_{bd}(k+1) + e^T(k+1)P_4 e(k+1) + o_1^2 + o_3^2 + o_4^2 + o_5^2 \\ &= \phi_1^T(k) (\Phi_1 + T_1^T P_1^{-1} T_1 + T_2^T P_2^{-1} T_2 + T_3^T P_3^{-1} T_3 + T_4^T P_4^{-1} T_4) \phi_1(k) + o_1^2 + o_3^2 + o_4^2 + o_5^2 \\ &= \phi_1^T(k)\Psi_1\phi_1(k) + o_1^2 + o_3^2 + o_4^2 + o_5^2. \end{aligned} \quad (43)$$

Case II: As for $ACK = 1, g(k) \geq 0$, by considering (25), (40) and (41), it can be got that

$$\begin{aligned} \Delta V(k) &\leq \bar{\delta}_2 \phi^T(k) C_{ar}^T \Omega_2 C_{ar} \phi(k) - \phi^T(k) E_3^T P_1 E_3 \phi(k) - r^T(k)r(k) - e_{ar}^T(k)P_2 e_{ar}(k) - e_{bd}^T(k)P_3 e_{bd}(k) \\ &\quad - e^T(k)P_4 e(k) - \varepsilon^T(k)\Omega_2\varepsilon(k) - \Delta r^T(k)\Delta r(k) - \Delta d^T(k)\Delta d(k) + \phi^T(k+1)E_3^T P_1 E_3 \phi(k+1) \\ &\quad + e_{ar}^T(k+1)P_2 e_{ar}(k+1) + e_{bd}^T(k+1)P_3 e_{bd}(k+1) + e^T(k+1)P_4 e(k+1) + r^T(k)r(k) \\ &\quad + \Delta r^T(k)\Delta r(k) + \Delta d^T(k)\Delta d(k) \\ &= \phi_2(k)^T(k)\Phi_2\phi_2(k) + \phi^T(k+1)E_3^T P_1 E_3 \phi(k+1) + e_{ar}^T(k+1)P_2 e_{ar}(k+1) \\ &\quad + e_{bd}^T(k+1)P_3 e_{bd}(k+1) + e^T(k+1)P_4 e(k+1) + o_1^2 + o_3^2 + o_4^2 \\ &= \phi_2^T(k) (\Phi_2 + T_5^T P_1^{-1} T_5 + T_6^T P_2^{-1} T_6 + T_7^T P_3^{-1} T_7 + T_8^T P_4^{-1} T_8) \phi_2(k) + o_1^2 + o_3^2 + o_4^2 \\ &= \phi_2^T(k)\Psi_2\phi_2(k) + o_1^2 + o_3^2 + o_4^2. \end{aligned} \quad (44)$$

Case III: As for $ACK = 0$, by combining (26), (40) and (41), it can be deduced that

$$\begin{aligned} \Delta V(k) &\leq \phi_2(k)^T(k)\Phi_3\phi_2(k) + \phi^T(k+1)E_3^T P_1 E_3 \phi(k+1) + e_{ar}^T(k+1)P_2 e_{ar}(k+1) \\ &\quad + e_{bd}^T(k+1)P_3 e_{bd}(k+1) + e^T(k+1)P_4 e(k+1) + o_1^2 + o_3^2 + o_4^2 \\ &= \phi_2^T(k) (\Phi_3 + T_9^T P_1^{-1} T_9 + T_{10}^T P_2^{-1} T_{10} + T_{11}^T P_3^{-1} T_{11} + T_{12}^T P_4^{-1} T_{12}) \phi_2(k) + o_1^2 + o_3^2 + o_4^2 \\ &= \phi_2^T(k)\Psi_3\phi_2(k) + o_1^2 + o_3^2 + o_4^2. \end{aligned} \quad (45)$$

Now, according to above discussions, by exploiting Lemma 2 and (38), one can obtain $\Psi_1 < 0, \Psi_2 < 0, \Psi_3 < 0$. On this basis, supposing a scalar γ such that $0 < \gamma < \min \{-\lambda_{\max}(\Psi_1), -\lambda_{\max}(\Psi_2), -\lambda_{\max}(\Psi_3)\}$, one can derive

$$\Delta V(k) \triangleq V(k+1) - V(k) \leq \frac{-\gamma}{\lambda_2} V(k) + o_1^2 + o_3^2 + o_4^2 + o_5^2. \quad (46)$$

Then it follows from (46) and Definition 1 that the augmented closed-loop system (24), (25) and (26) is uniformly ultimately bounded. Especially, the upper bound is $\sqrt{\frac{\lambda_2(o_1^2 + o_3^2 + o_4^2 + o_5^2) + \gamma \varepsilon}{\gamma \lambda_1}}$, where ε is an arbitrarily small positive number. It completes the proof.

Remark 6. This paper initially utilizes the ACK concept to identify the occurring intervals of DoS attacks. Then, as for the sleep intervals of the DoS attacks, the convention ETS and memory one are combined to design the switching-like ETS, which can achieve a good balance between reduced data transmissions and desirable performance. In (43), as for the coupling terms

$e_{ar}^T(k-i)e_{ar}(k-j)$ ($i \neq j$), it is assumed that there exists an upper bound σ_2^2 on these couplings, which is reasonable according to the definition of $e_{ar}(k) = [e_{x_a}^T(k), e_r^T(k)]^T$.

From Theorem 2, it can be easily checked that there exist some nonlinear terms such as $P_2 L_{ar}$, $P_3 L_{bd}$, $P_4 \bar{B}_b K_1$ and $P_4 \bar{B}_b K_2$, and these couplings make the inequalities (38) uneasily tested by using the Matlab LMI Toolbox. Therefore, an easy-to-test theorem needs to be presented in what follows.

Theorem 3. For some given positive constants $o_1, o_2, o_3, o_4, o_5, \bar{\delta}_1, \bar{\delta}_2, \delta_3, p_i$ ($i = 0, \dots, m-1$) and matrices $S_b, K_a, K_b, K_r, K_d, K_1, K_2$ are obtained by (3) and Assumption 2, under the switching-like ETS scheme (13), the observer (14), (16) with the observer gains $L_{ar} = P_2^{-1} X_1$, $L_{bd} = P_3^{-1} X_2$, $\bar{L}_{ar} = P_2^{-1} X_3$ and the tracking controller (21) with controller gain $K_1 = Z_1^{-1} J_1$, $K_2 = Z_2^{-1} J_2$, the UAH system and the UGV one can realize the desirable tracking control target, if there exist matrices $P_1 > 0$, $P_2 > 0$, $P_3 > 0$, $P_4 > 0$, $\Omega_1 > 0$, $\Omega_2 > 0$, $\Omega_3 > 0$, Z_1, Z_2, J_1, J_2 with appropriate dimensions, and scalars $\sigma_1 > 0$, $\sigma_2 > 0$, $\sigma_3 > 0$ such that the following LMIs satisfy

$$\Xi_1 = \begin{bmatrix} \Xi_1^{11} & \Xi_1^{12} & \Xi_1^{13} & 0 \\ * & \Xi_1^{22} & 0 & 0 \\ * & * & \Xi_1^{33} & \Xi_1^{34} \\ * & * & * & \Xi_1^{44} \end{bmatrix} < 0, \quad \Xi_2 = \begin{bmatrix} \Xi_2^{11} & \Xi_2^{12} & \Xi_2^{13} & 0 \\ * & \Xi_2^{22} & 0 & 0 \\ * & * & \Xi_2^{33} & \Xi_2^{34} \\ * & * & * & \Xi_2^{44} \end{bmatrix} < 0, \quad \Xi_3 = \begin{bmatrix} \Xi_3^{11} & \Xi_3^{12} & \Xi_3^{13} & 0 \\ * & \Xi_3^{22} & 0 & 0 \\ * & * & \Xi_3^{33} & \Xi_3^{34} \\ * & * & * & \Xi_3^{44} \end{bmatrix} < 0, \quad (47)$$

where

$$\begin{aligned} \Xi_1^{11} &= \Phi_1, \quad \Xi_2^{11} = \Phi_2, \quad \Xi_3^{11} = \Phi_3, \quad \Xi_1^{12} = [S_1^T, S_2^T, S_3^T, S_4^T], \quad \Xi_2^{12} = [S_5^T, S_6^T, S_7^T, S_8^T], \\ \Xi_3^{12} &= [S_9^T, S_{10}^T, S_{11}^T, S_{12}^T], \quad \Xi_1^{13} = [0, \bar{B}_b^T \bar{B}_b J_1 E_3, 0, \dots, 0, -\bar{B}_b^T \bar{B}_b J_1 S_b E_4, \bar{B}_b^T \bar{B}_b J_1, 0, 0, 0]^T, \\ \Xi_2^{13} &= [0, \bar{B}_b^T \bar{B}_b J_1 E_3, -\bar{B}_b^T \bar{B}_b J_1 S_b E_4, \bar{B}_b^T \bar{B}_b J_1, 0, 0, 0]^T, \quad \Xi_3^{13} = [0, \bar{B}_b^T \bar{B}_b J_2 E_3, -\bar{B}_b^T \bar{B}_b J_2 S_b E_4, \bar{B}_b^T \bar{B}_b J_2, 0, 0, 0]^T, \\ \Xi_1^{22} &= \text{diag}(-P_1, -P_2, -P_3, -P_4 + \sigma_1 I_2), \quad \Xi_2^{22} = \text{diag}(-P_1, -P_2, -P_3, -P_4 + \sigma_2 I_2), \\ \Xi_3^{22} &= \text{diag}(-P_1, -P_2, -P_3, -P_4 + \sigma_3 I_2), \quad \Xi_1^{33} = \Xi_2^{33} = \text{He}\{-\bar{B}_b^T \bar{B}_b Z_1\}, \quad \Xi_3^{33} = \text{He}\{-\bar{B}_b^T \bar{B}_b Z_2\}, \\ \Xi_1^{34} &= \Xi_2^{34} = U_1 = U_2 = P_4 \bar{B}_b - \bar{B}_b Z_1, \quad \Xi_3^{34} = U_3 = P_4 \bar{B}_b - \bar{B}_b Z_2, \quad \Xi_1^{44} = -\sigma_1 I_2, \quad \Xi_2^{44} = -\sigma_2 I_2, \quad \Xi_3^{44} = -\sigma_3 I_2, \end{aligned}$$

with

$$\begin{aligned} S_1 &= [P_1 E_3 A_{ar}, 0, 0, \dots, 0, 0, 0, 0, 0], \\ S_2 &= [0, p_0^2 P_2 A_{ar} - p_0^2 X_1 C_{ar}, -p_0^2 p_1 X_1 C_{ar}, \dots, -p_0^2 p_{m-1} X_1 C_{ar}, 0, 0, X_1, P_2 E_1, 0], \\ S_3 &= [0, 0, 0, \dots, 0, P_3 A_{bd} - X_2 C_{bd}, 0, 0, 0, P_3 E_2], \quad S_4 = [0, S_4^1, 0, \dots, 0, S_4^2, S_4^3, 0, 0, 0], \\ S_4^1 &= \bar{B}_b J_1 E_3 - P_4 \bar{B}_b K_r E_1^T, \quad S_4^2 = P_4 \bar{B}_b K_d E_2^T - P_4 \bar{B}_b K_b E_4 - \bar{B}_b J_1 S_b E_4, \quad S_4^3 = P_4 \bar{A}_a + \bar{B}_b J_1, \\ S_5 &= [P_1 E_3 A_{ar}, 0, 0, 0, 0, 0, 0], \quad S_6 = [0, P_2 A_{ar} - X_1 C_{ar}, 0, 0, X_1, P_2 E_1, 0], \\ S_7 &= [0, 0, P_3 A_{bd} - X_2 C_{bd}, 0, 0, 0, P_3 E_2], \quad S_8 = [0, S_8^1, S_8^2, S_8^3, 0, 0, 0], \\ S_8^1 &= S_4^1, \quad S_8^2 = S_4^2, \quad S_8^3 = S_4^3, \quad S_9 = S_5, \quad S_{10} = [0, P_2 A_{ar} - X_3 C_{ar}, 0, 0, X_3, P_2 E_1, 0], \\ S_{11} &= S_7 S_{12} = [0, S_{12}^1, S_{12}^2, S_{12}^3, 0, 0, 0], \quad S_{12}^1 = \bar{B}_b J_2 E_3 - P_4 \bar{B}_b K_r E_1^T, \\ S_{12}^2 &= P_4 \bar{B}_b K_d E_2^T - P_4 \bar{B}_b K_b E_4 - \bar{B}_b J_2 S_b E_4, \quad S_{12}^3 = P_4 \bar{A}_a + \bar{B}_b J_2. \end{aligned}$$

Proof. Initially, these coupling terms in Theorem 2 are denoted as follows

$$P_2 L_{ar} = X_1, \quad P_3 L_{bd} = X_2, \quad P_2 \bar{L}_{ar} = X_3, \quad K_1 = Z_1^{-1} J_1, \quad K_2 = Z_2^{-1} J_2. \quad (48)$$

In order to facilitate the following derivation, these inequalities in (38) can be rewritten as follows

$$\begin{aligned} \Xi_1 &= \begin{bmatrix} \Xi_1^{11} & \Xi_1^{12} \\ * & \Gamma_1^{22} \end{bmatrix} + \text{He} \left\{ \begin{bmatrix} \vartheta_1 \\ \vartheta_2 \end{bmatrix} U_1 V_1 \begin{bmatrix} \vartheta_3 & \vartheta_4 \end{bmatrix} \right\} < 0, \\ \Xi_2 &= \begin{bmatrix} \Xi_2^{11} & \Xi_2^{12} \\ * & \Gamma_2^{22} \end{bmatrix} + \text{He} \left\{ \begin{bmatrix} \vartheta_5 \\ \vartheta_6 \end{bmatrix} U_2 V_2 \begin{bmatrix} \vartheta_7 & \vartheta_8 \end{bmatrix} \right\} < 0, \\ \Xi_3 &= \begin{bmatrix} \Xi_3^{11} & \Xi_3^{12} \\ * & \Gamma_3^{22} \end{bmatrix} + \text{He} \left\{ \begin{bmatrix} \vartheta_5 \\ \vartheta_6 \end{bmatrix} U_3 V_3 \begin{bmatrix} \vartheta_7 & \vartheta_8 \end{bmatrix} \right\} < 0, \end{aligned} \quad (49)$$

where

$$\begin{aligned} \vartheta_1 &= 0_{(26+4m+3w) \times 2}, \quad \vartheta_2 = I_2, \quad \vartheta_3 = I_{(16+4m+2w)}, \quad \vartheta_4 = 0_{(16+4m+2w) \times (12+w)}, \\ \vartheta_5 &= 0_{(30+3w) \times 2}, \quad \vartheta_6 = I_2, \quad \vartheta_7 = I_{(20+2w)}, \quad \vartheta_8 = 0_{(20+2w) \times (12+w)}, \\ U_1 &= U_2 = P_4 \bar{B}_b - \bar{B}_b Z_1, \quad U_3 = P_4 \bar{B}_b - \bar{B}_b Z_2, \\ V_1 &= [0, Z_1^{-1} J_1 E_3, \underbrace{0, \dots, 0}_{m-1}, -Z_1^{-1} J_1 S_b E_4, Z_1^{-1} J_1, 0, 0, 0], \\ V_2 &= [0, Z_1^{-1} J_1 E_3, -Z_1^{-1} J_1 S_b E_4, Z_1^{-1} J_1, 0, 0, 0], \\ V_3 &= [0, Z_2^{-1} J_2 E_3, -Z_2^{-1} J_2 S_b E_4, Z_2^{-1} J_2, 0, 0, 0]. \end{aligned}$$

Then, according to Lemma 4, there must exist the scalars σ_i ($i = 1, 2, 3$) such that the following formulas hold

$$\begin{aligned} \text{He} \left\{ \begin{bmatrix} \vartheta_1 \\ \vartheta_2 \end{bmatrix} U_1 V_1 \begin{bmatrix} \vartheta_3 & \vartheta_4 \end{bmatrix} \right\} &\leq \sigma_1 \begin{bmatrix} \vartheta_1 \\ \vartheta_2 \end{bmatrix} \begin{bmatrix} \vartheta_1^T & \vartheta_2^T \end{bmatrix} + \sigma_1^{-1} \begin{bmatrix} \vartheta_3^T \\ \vartheta_4^T \end{bmatrix} V_1^T U_1^T U_1 V_1 \begin{bmatrix} \vartheta_3 & \vartheta_4 \end{bmatrix}, \\ \text{He} \left\{ \begin{bmatrix} \vartheta_5 \\ \vartheta_6 \end{bmatrix} U_2 V_2 \begin{bmatrix} \vartheta_7 & \vartheta_8 \end{bmatrix} \right\} &\leq \sigma_2 \begin{bmatrix} \vartheta_5 \\ \vartheta_6 \end{bmatrix} \begin{bmatrix} \vartheta_5^T & \vartheta_6^T \end{bmatrix} + \sigma_2^{-1} \begin{bmatrix} \vartheta_7^T \\ \vartheta_8^T \end{bmatrix} V_2^T U_2^T U_2 V_2 \begin{bmatrix} \vartheta_7 & \vartheta_8 \end{bmatrix}, \\ \text{He} \left\{ \begin{bmatrix} \vartheta_5 \\ \vartheta_6 \end{bmatrix} U_3 V_3 \begin{bmatrix} \vartheta_7 & \vartheta_8 \end{bmatrix} \right\} &\leq \sigma_3 \begin{bmatrix} \vartheta_5 \\ \vartheta_6 \end{bmatrix} \begin{bmatrix} \vartheta_5^T & \vartheta_6^T \end{bmatrix} + \sigma_3^{-1} \begin{bmatrix} \vartheta_7^T \\ \vartheta_8^T \end{bmatrix} V_3^T U_3^T U_3 V_3 \begin{bmatrix} \vartheta_7 & \vartheta_8 \end{bmatrix}. \end{aligned} \quad (50)$$

Combining (49) and (50) with the definition of Schur-complement yields

$$\begin{aligned} \begin{bmatrix} \Xi_1^{11} & \Xi_1^{12} \\ * & \Gamma_1^{22} \end{bmatrix} + \sigma_1 \begin{bmatrix} \vartheta_1 \\ \vartheta_2 \end{bmatrix} \begin{bmatrix} \vartheta_1^T & \vartheta_2^T \end{bmatrix} + \sigma_1^{-1} \begin{bmatrix} \vartheta_3^T \\ \vartheta_4^T \end{bmatrix} V_1^T U_1^T U_1 V_1 \begin{bmatrix} \vartheta_3 & \vartheta_4 \end{bmatrix} &< 0, \\ \begin{bmatrix} \Xi_2^{11} & \Xi_2^{12} \\ * & \Gamma_2^{22} \end{bmatrix} + \sigma_2 \begin{bmatrix} \vartheta_5 \\ \vartheta_6 \end{bmatrix} \begin{bmatrix} \vartheta_5^T & \vartheta_6^T \end{bmatrix} + \sigma_2^{-1} \begin{bmatrix} \vartheta_7^T \\ \vartheta_8^T \end{bmatrix} V_2^T U_2^T U_2 V_2 \begin{bmatrix} \vartheta_7 & \vartheta_8 \end{bmatrix} &< 0, \\ \begin{bmatrix} \Xi_3^{11} & \Xi_3^{12} \\ * & \Gamma_3^{22} \end{bmatrix} + \sigma_3 \begin{bmatrix} \vartheta_5 \\ \vartheta_6 \end{bmatrix} \begin{bmatrix} \vartheta_5^T & \vartheta_6^T \end{bmatrix} + \sigma_3^{-1} \begin{bmatrix} \vartheta_7^T \\ \vartheta_8^T \end{bmatrix} V_3^T U_3^T U_3 V_3 \begin{bmatrix} \vartheta_7 & \vartheta_8 \end{bmatrix} &< 0, \end{aligned} \quad (51)$$

such that

$$\begin{bmatrix} \Xi_1^{11} & \Xi_1^{12} & 0 \\ * & \Xi_1^{22} & V_1 \\ * & * & -(\sigma_1^{-1} U_1^T U_1)^{-1} \end{bmatrix} < 0, \quad \begin{bmatrix} \Xi_2^{11} & \Xi_2^{12} & 0 \\ * & \Xi_2^{22} & V_2 \\ * & * & -(\sigma_2^{-1} U_2^T U_2)^{-1} \end{bmatrix} < 0, \quad \begin{bmatrix} \Xi_3^{11} & \Xi_3^{12} & 0 \\ * & \Xi_3^{22} & V_3 \\ * & * & -(\sigma_3^{-1} U_3^T U_3)^{-1} \end{bmatrix} < 0. \quad (52)$$

By employing Lemma 3 and Schur-complement once again, (52) is rewritten as

$$\begin{bmatrix} \Pi_1 & \bar{\bar{B}}_1 V_1 & 0 \\ * & 0 & 0 \\ * & \Xi_1^{33} & U_1 \\ * & * & -\sigma_1 I_2 \end{bmatrix} < 0, \quad \begin{bmatrix} \Pi_2 & \bar{\bar{B}}_2 V_2 & 0 \\ * & 0 & 0 \\ * & \Xi_2^{33} & U_2 \\ * & * & -\sigma_2 I_2 \end{bmatrix} < 0, \quad \begin{bmatrix} \Pi_3 & \bar{\bar{B}}_3 V_3 & 0 \\ * & 0 & 0 \\ * & \Xi_3^{33} & U_3 \\ * & * & -\sigma_3 I_2 \end{bmatrix} < 0, \quad (53)$$

where $\Pi_1 = \begin{bmatrix} \Xi_1^{11} & \Xi_1^{12} \\ * & \Xi_1^{22} \end{bmatrix}$, $\Pi_2 = \begin{bmatrix} \Xi_2^{11} & \Xi_2^{12} \\ * & \Xi_2^{22} \end{bmatrix}$, $\Pi_3 = \begin{bmatrix} \Xi_3^{11} & \Xi_3^{12} \\ * & \Xi_3^{22} \end{bmatrix}$, $\bar{\bar{B}}_1 = \bar{B}_b^T \bar{B}_b Z_1$, $\bar{\bar{B}}_2 = \bar{B}_b^T \bar{B}_b Z_2$. Then it follows from (53) that the inequalities in Theorem 2-3 are equivalent, and the proof is completed.

Remark 7. Based on Theorems 1-3, the novelties of this work can be summarized in three points. Firstly, by utilizing the ACK to define whether the DoS attacks occur or not, a switching-like ETS is proposed to reject such cyber-attack and achieve good balance between less data transmissions and ideal tracking performance. Secondly, by designing the corresponding observers with switchable gains or constant ones, an anti-disturbance tracking controller is presented based on the estimations of disturbance and reference signal, tracking error, and ACK concept, which can compensate for the negative impacts of disturbance and DoS attacks. Thirdly, a co-design method of checking the observer gains, controller gains, and trigger parameters is established in the form of the LMIs, which can be easily tested and applied to real UAH/UGV systems.

4 | SIMULATION EXPERIMENT

In this section, a simulated example is presented to verify the effectiveness and advantage of our tracking control scheme on the basis of two cases.

Initially, by referring to³⁴ and³⁵, and setting sampling period $h = 0.02s$, the parameters of UAH/UGV systems in (1)-(2) are presented as follows

$$A_a = \begin{bmatrix} 1 & 0 \\ 0 & 1 \end{bmatrix}, B_a = \begin{bmatrix} 0.02 & 0 \\ 0 & 0.02 \end{bmatrix}, B_r = \begin{bmatrix} 0.02 & 0 \\ 0 & 0.02 \end{bmatrix}, C_a = \begin{bmatrix} 1 & 0 \\ 0 & 1 \end{bmatrix}, C_b = \begin{bmatrix} 1 & 0 & 0 & 0 \\ 0 & 0 & 1 & 0 \end{bmatrix},$$

$$A_b = \begin{bmatrix} 1 & 0.02 & 0 & 0 \\ 0 & 1 & 0 & 0 \\ 0 & 0 & 1 & 0.02 \\ 0 & 0 & 0 & 1 \end{bmatrix}, B_b = B_d = \begin{bmatrix} -0.002 & 0 \\ -0.2 & 0 \\ 0 & 0.002 \\ 0 & 0.2 \end{bmatrix}.$$

Then, the external disturbance is described as

$$d_1(k) = \sin\left(\frac{k\pi}{100}\right) + 0.5\sin\left(\frac{k\pi}{50}\right) + 0.25\sin\left(\frac{k\pi}{25}\right) + \cos\left(\frac{k\pi}{100}\right) + 0.5\cos\left(\frac{k\pi}{50}\right) + 0.25\cos\left(\frac{k\pi}{25}\right),$$

$$d^T(k) = [d_1(k) \quad -d_1(k)].$$

In virtue of Assumption 2, part parameters of the UGV controller in (3) and the UAH controller in (21) are calculated as

$$K_a = \begin{bmatrix} -5 & 0 \\ 0 & -5 \end{bmatrix}, K_b = \begin{bmatrix} 50 & 10 & 0 & 0 \\ 0 & 0 & -50 & -10 \end{bmatrix}, K_r = \begin{bmatrix} -10 & 0 \\ 0 & 10 \end{bmatrix}, K_d = \begin{bmatrix} 1 & 0 \\ 0 & 1 \end{bmatrix}, S_b = \begin{bmatrix} 1 & 0 & 0 & 0 \\ 0 & 0 & 1 & 0 \end{bmatrix}.$$

Based on Theorem 1, by setting $\bar{\delta}_1 = 0.0025$, $\bar{\delta}_2 = 0.0049$, and $\delta_3 = 0.0009$, the maximum allowable number of packets losses can be obtained as $M = 3$ when solving the inequations in (27).

Now, as for the switching-like ETS, we choose these parameters as $m = 2$, $p_0 = 0.7$, $p_1 = 0.3$. Then, by solving the LMIs in Theorem 3, the triggered matrices of the ETS $\Omega_1, \Omega_2, \Omega_3$, the observer gains $L_{11}, L_{21}, L_{12}, L_{22}, L_3, L_4$, the controller gains K_1, K_2 , and the constants $\sigma_1, \sigma_2, \sigma_3$ are computed out as

$$\Omega_1 = \begin{bmatrix} 47.4877 & 0 & 0.5824 & 0 \\ 0 & 47.4877 & 0 & 0.5824 \\ 0.5824 & 0 & 42.6049 & 0 \\ 0 & 0.5824 & 0 & 42.6049 \end{bmatrix}, \Omega_2 = \begin{bmatrix} 47.0944 & 0 & -0.4530 & 0 \\ 0 & 47.0944 & 0 & -0.4530 \\ -0.4530 & 0 & 38.0911 & 0 \\ 0 & -0.4530 & 0 & 38.0911 \end{bmatrix},$$

$$\Omega_3 = \begin{bmatrix} 49.9534 & 0 & -0.0787 & 0 \\ 0 & 49.9534 & 0 & -0.0787 \\ -0.0787 & 0 & 42.3455 & 0 \\ 0 & -0.0787 & 0 & 42.3455 \end{bmatrix}, L_{11} = \begin{bmatrix} 0.4713 & 0 \\ 0 & 0.4713 \end{bmatrix}, L_{21} = \begin{bmatrix} 0.9902 & 0 \\ 0 & 0.9902 \end{bmatrix},$$

$$L_{12} = \begin{bmatrix} 0.3685 & 0 \\ 0 & 0.3685 \end{bmatrix}, L_{22} = \begin{bmatrix} 0.9374 & 0 \\ 0 & 0.9374 \end{bmatrix}, L_3 = \begin{bmatrix} 1.3955 & 21.5293 & 0 & 0 \\ 0 & 0 & 1.3955 & 21.5293 \end{bmatrix}^T,$$

$$L_4 = \begin{bmatrix} -18.1056 & 0 \\ 0 & 18.1056 \end{bmatrix}, K_1 = \begin{bmatrix} -0.1839 & 0 \\ 0 & -0.1839 \end{bmatrix}, K_2 = \begin{bmatrix} -0.0024 & 0 \\ 0 & -0.0024 \end{bmatrix},$$

$$\sigma_1 = 0.5707, \sigma_2 = 0.4265, \sigma_3 = 0.5713.$$

Meanwhile, by defining the vectors $e_x(k) = x_{bx}(k) - x_{ax}(k)$, $e_y(k) = x_{by}(k) - x_{ay}(k)$, and the total number of samples N , some performance evaluation functions are put forward to evaluate the tracking control performance between our ETS and existent ones,

$$S_x = \sqrt{\left(\sum_{k=1}^N |e_x(k)|\right)/N}, S_y = \sqrt{\left(\sum_{k=1}^N |e_y(k)|\right)/N}, S_{xy} = \sqrt{\left(\sum_{k=1}^N |e_x(k)| + |e_y(k)|\right)/N}. \quad (54)$$

Case I. The reference trajectory $r(k) = [r_{x_1}(k), r_{y_1}(k)]^T$ of the UGV system is selected as the following planar ellipse

$$\begin{cases} r_{x_1}(k) = 500\cos\left(\frac{k+1}{25\pi} + \frac{3}{2}\right) - 450\cos\left(\frac{k}{25\pi}\right), \\ r_{y_1}(k) = 500\sin\left(\frac{k+1}{25\pi} + \frac{3}{2}\right) - 450\sin\left(\frac{k}{25\pi}\right). \end{cases}$$

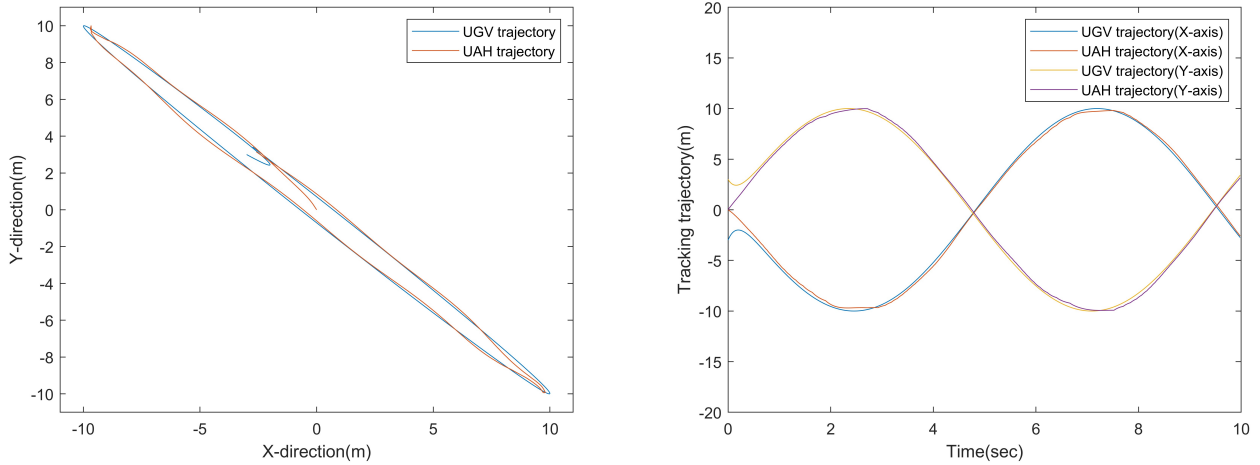


FIGURE 4 Track tracking curves of the UGV and the UAH.

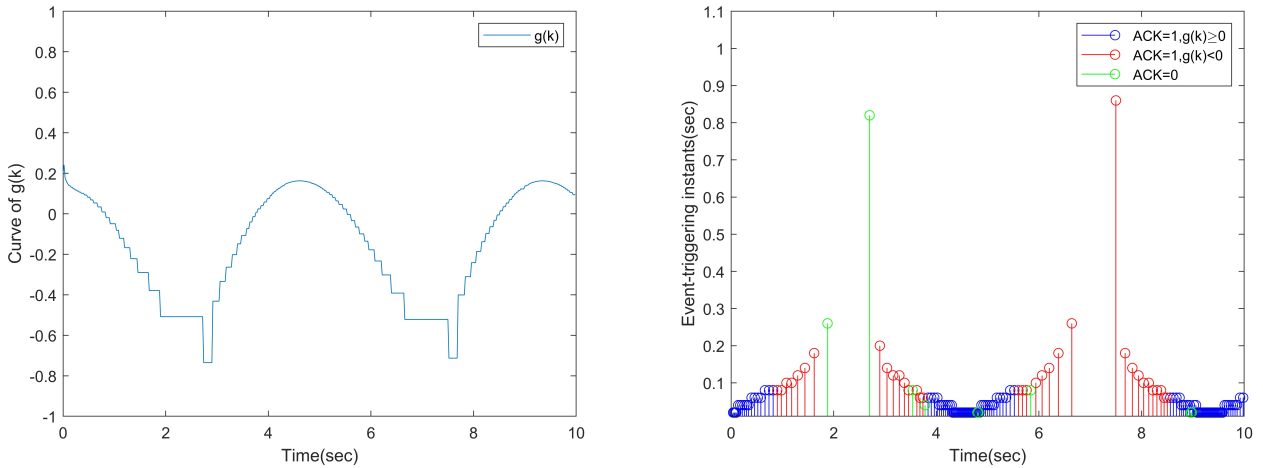


FIGURE 5 Curve of $g(k)$ and triggered time interval of the switching-like ETS.

TABLE 1 The effects of different β on the switching-like ETS (Case I)

Parameter β	Transmitted packets				S_x	S_y	S_{xy}
	METS	CETS	FETS	Total			
0.6	12	130	6	148	0.5423	0.5338	0.7609
0.7	21	123	6	150	0.5390	0.5281	0.7546
0.8	35	111	12	158	0.5342	0.5241	0.7483
0.9	61	90	15	166	0.5360	0.5247	0.7497

By setting the initial values as $x_a(0) = [-3, 3]^T$, $x_b(0) = [0, 0, 0, 0]^T$, $g(0) = 0.2$ and $\beta = 0.8$, then the simulation results are shown in Figs. 4, 5, and 6.

Fig. 4 illustrates the overall trajectory tracking curves of the UAH/UGV systems (left), in which the blue line is the trajectory of the UGV and the red line is the trajectory of the UAH. Besides the trajectory curves of the UAH/UGV systems in X and Y directions are also presented in Fig. 4 (right), respectively. It can be seen that under our proposed control scheme, the UAH can effectively track the reference trajectory of the UGV. The change of the switching function $g(k)$ (left) and the triggered intervals

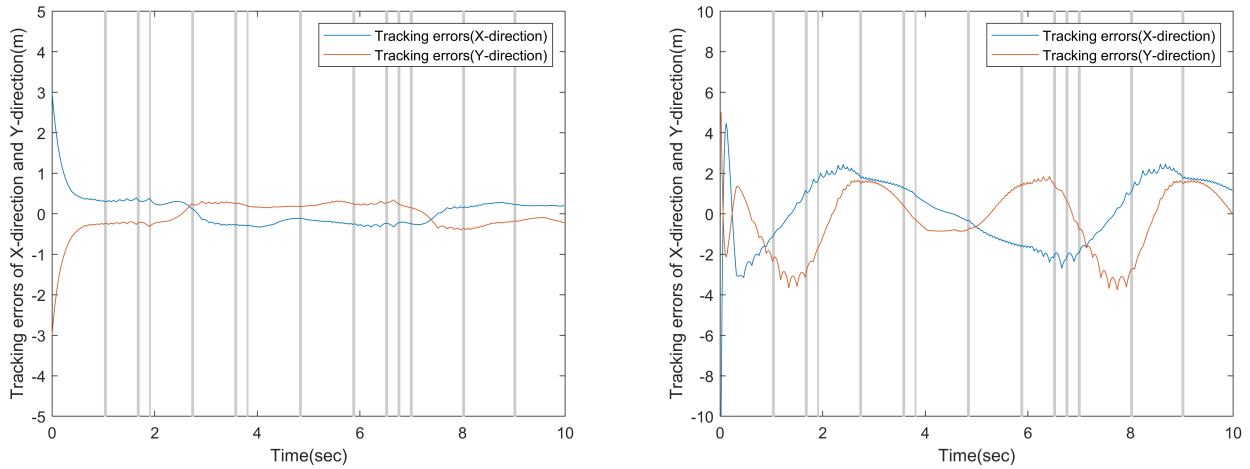


FIGURE 6 Trajectory error curve of the UAH tracking the UGV under the DoS attacks in X -direction and Y -direction.

TABLE 2 The comparisons of three different ETSs and $\beta = 0.8$ (Case I)

	Type of event-triggered scheme	Transmitted packets	S_x	S_y	S_{xy}
Case (1)	Switching-like ETS ($\bar{\delta}_1 = 0.0025, \bar{\delta}_2 = 0.0049$)	158	0.5342	0.5241	0.7483
	Memory ETS ($\bar{\delta}_1 = 0.0025$)	175	0.5415	0.5283	0.7565
	Conventional ETS ($\bar{\delta}_2 = 0.0049$)	141	0.5459	0.5377	0.7662
Case (2)	Switching-like ETS ($\bar{\delta}_1 = 0.0036, \bar{\delta}_2 = 0.0064$)	144	0.5496	0.5444	0.7736
	Memory ETS ($\bar{\delta}_1 = 0.0036$)	142	0.5525	0.5464	0.7770
	Conventional ETS ($\bar{\delta}_2 = 0.0064$)	130	0.5445	0.5533	0.7763

of the ETS (right) are respectively given in Fig. 5. Fig. 6 (left) depicts the trajectory tracking error curve under the DoS attacks and outside disturbance.

Now, the performance evaluation functions in (54) is used to compare the effects with different β in the switching-like ETS, which are shown in Table 1. In this table, the METS, CETS and FETS represent the data packets transmitted by memory ETS, conventional ETS, and fixed threshold ETS, respectively. By increasing β , the number of transmitted packets by memory ETS becomes larger, while the one by conventional ETS decreases, resulting in an increasing number of data packets triggered by switching-like ETS, but the control performance is improved. Moreover, from Table 1, it is worth noting that the bettering of control performance is not necessarily accompanied with the increasing transmitted packets. By setting $\beta = 0.9$ as an example, the main reason is that the erroneous triggers and repeated ones are caused by the memory ETS. This situation should be avoided by decreasing β for switching to the conventional ETS in the peak or trough phase of the composite signal.

In addition, by keeping the same parameters, some comparisons are presented among the switching-like ETS, conventional ETS, and memory ETS in two situations. Based on three above ETSs, the transmitted packets and control performance are illustrated in Table 2. It follows from Table 2 that, as for Case (1), the tracking performance induced by our switching-like ETS is the best among three ETSs, and the data transmissions remains intermediate between the conventional ETS and memory ETS. However, in Case (2), it is important to choose the suitable upper bounds of the triggered thresholds $\bar{\delta}_1$ and $\bar{\delta}_2$. Under the Theorem 1, a reasonable selection of $\bar{\delta}_i$ ($i = 1, 2$) can ensure that the memory ETS operates at the peak and trough of the signal $\rho_y(k)$, while the conventional ETS works at rapid changes of $\rho_y(k)$, which can help to achieve the desirable performance. Otherwise, the unsuitable selections $\bar{\delta}_i$ ($i = 1, 2$) lead to the opposite results.

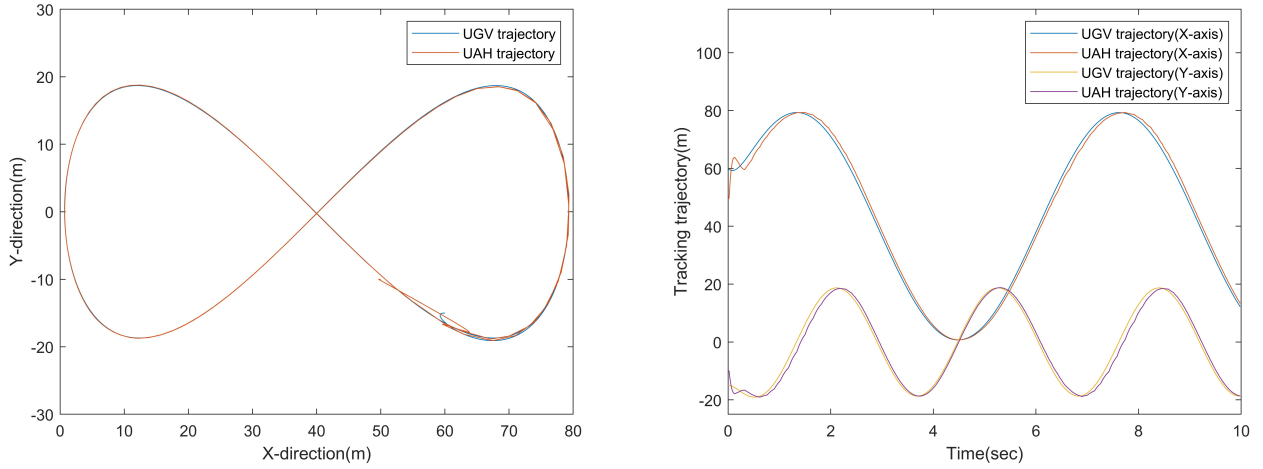


FIGURE 7 Trajectory curves of the UGV and the UAH.

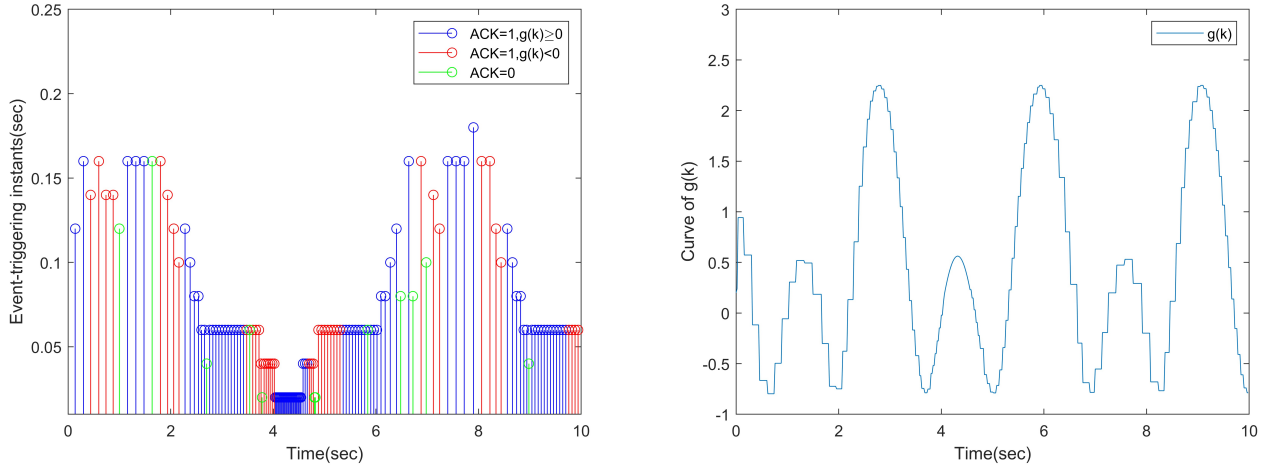


FIGURE 8 Event-triggering instants of the switching-like ETS and curve of $f(k)$.

TABLE 3 The effects of different β on the switching-like switching-like ETS (Case II)

Parameter β	Transmitted packets				S_x	S_y	S_{xy}
	METS	CETS	FETS	Total			
3	23	110	10	143	1.2297	1.1832	1.7065
3.5	41	92	12	145	1.2110	1.1666	1.6815
4	74	63	20	157	1.1960	1.1375	1.6506
4.5	99	40	24	163	1.1879	1.1171	1.6306

Case II. In order to further verify the efficiency and superiority of our proposed ETS, an eight curve shape trajectory, in which a new reference $r(k) = [r_{x_2}(k), r_{y_2}(k)]^T$ is added into the $X - Y$ plane, is proposed as follows

$$\begin{cases} r_{x_2}(k) = 200(1 - \cos(2k)), \\ r_{y_2}(k) = 100\sin(4k). \end{cases}$$

TABLE 4 The comparisons of three different ETSs and $\beta = 3.5$ (Case II)

	Type of event-triggered scheme	Transmitted packets	S_x	S_y	S_{xy}
Case (3)	Switching-like ETS ($\bar{\delta}_1 = 0.0025, \bar{\delta}_2 = 0.0049$)	145	1.2110	1.1666	1.6815
	Memory ETS ($\bar{\delta}_1 = 0.0025$)	158	1.1638	1.0981	1.6001
	Conventional ETS ($\bar{\delta}_2 = 0.0049$)	133	1.2648	1.1967	1.7412
Case (4)	Switching-like ETS ($\bar{\delta}_1 = 0.0036, \bar{\delta}_2 = 0.0064$)	136	1.2631	1.2111	1.7499
	Memory ETS ($\bar{\delta}_1 = 0.0036$)	135	1.2182	1.1479	1.6739
	Conventional ETS ($\bar{\delta}_2 = 0.0064$)	122	1.3242	1.2460	1.8183

By setting initial values as $x_a(0) = [60, -15]^T$, $x_b(0) = [50, 0, -10, 0]^T$, $g(0) = 0.1$ and $\beta = 3.5$, then some simulation results are displayed in Figs. 6, 7 and 8.

The simulation diagram concerning tracking trajectory results by our switching-like ETS is shown in Fig. 6 and Fig. 7. Fig. 6 (right) depicts the trajectory error curves of UAH/UGV systems under the DoS attacks and disturbance. Fig. 7 (left) shows the overall trajectory tracking curves of the UAH/UGV systems, and Fig. 7 (right) represents the trajectory curves in X and Y direction, respectively. The event-triggering intervals and the switching function $g(k)$ are shown in Fig. 8, respectively. Besides, the effectiveness of our switching-like ETS in the tracking control can be testified in the Fig. 7 and Fig. 8. Moreover, the effects of selecting different β are given in Table 3. From Table 3, we choose $\beta = 3.5$ to give the following comparison since better balance between less data transmissions and ideal performance are achieved, which can be shown in Table 4. From Table 4, it is easy to see that our switching-like ETS can be more effective than the conventional ETS and the memory ETS by choosing the suitable triggered thresholds $\bar{\delta}_1$ and $\bar{\delta}_2$.

5 | CONCLUSIONS

In this paper, an anti-disturbance trajectory tracking control scheme based on the switching-like adaptive ETS for the UAH/UGV systems with unavailable state, external disturbance, and DoS attacks has been proposed. Firstly, a new type of switching-like ETS was presented, which could include the conventional ETS and memory ETS switched by a designed switching function, to maintain desirable control performance and less data transmissions, and effectively restrain the DoS attacks. Secondly, the ACK concept was pointed out to determine whether the active intervals or the sleep ones occur or not for the DoS attacks. Thirdly, an appropriate ETS was exploited that the switching-like adaptive ETS could be used for sleep intervals and the fixed trigger-threshold ETS aimed to tackle active ones. Fourthly, together with the observations and tracking error, an anti-disturbance tracking controller was designed and an augmented closed-loop system was established. Then, by using Lyapunov stability theory, a sufficient condition on uniform ultimate bounded stability was derived and a co-design method of checking the existence of observers, controller, and ETS was presented via a set of LMIs. Finally, some simulations and comparisons have been presented to illustrate the efficiency and validity of the proposed control scheme.

ACKNOWLEDGEMENTS

This work was supported by the National Natural Science Foundations of China (Nos. 62073164, 61922042), and the Project of Key Research & Development Plan of Jiangsu Province (No.BE2021016-5)

References

1. Gu X, Xian B and Wang Y. Agile flight for a quadrotor via robust geometry control: theory and experimental verification. *International Journal of Robust and Nonlinear Control*. 2022; 32(7): 4236-4250.

2. Yan K, Chen M, Wu Q and Wang Y. Adaptive flight control for unmanned autonomous helicopter with external disturbance and actuator fault. *The Journal of Engineering*. 2019; 8359-8364.
3. Vilchis JCA, Brogliato B, Dzul A and Lozano R. Nonlinear modelling and control of helicopters. *Automatica*. 2003; 39(10): 1583-1596.
4. Xian B and Yang S. Robust tracking control of a quadrotor unmanned aerial vehicle-suspended payload system. *IEEE/ASME Transactions on Mechatronics*. 2021; 26(5): 2653-2663.
5. Yan K and Wu QX. Adaptive tracking flight control for unmanned autonomous helicopter with full state constraints and actuator faults. *ISA Transactions*. 2022; 128(B): 32-46.
6. Meng W, He ZR, Su R, Yadav PK, Teo R and Xie LH. Decentralized multi-UAV flight autonomy for moving convoys search and track. *IEEE Transactions on Control Systems Technology*. 2017; 25(4): 1480-1487.
7. Pan ZH, Xia YQ, Sun ZQ and Yu TT. Multilayer self-organized aggregation control for large-scale unmanned aerial vehicle swarms. *International Journal of Robust and Nonlinear Control*. 2023; 1-17.
8. Liu DQ, Bao WD, Zhu XM, Fei BW, Xiao ZL and Men T. Vision-aware air-ground cooperative target localization for UAV and UGV. *Aerospace Science and Technology*. 2022; 124: 107525-107539.
9. Li JQ, Sun T, Huang XP, Ma LJ, Lin QZ, Chen J and Leung VCM. A memetic path planning algorithm for unmanned air/ground vehicle cooperative detection systems. *IEEE Transactions on Automation Science and Engineering*. 2022; 19(4): 2724-2737.
10. Ren Y, Zhang K, Jiang B, Cheng W and Ding Y. Distributed fault-tolerant time-varying formation control of heterogeneous multi-agent systems. *International Journal of Robust and Nonlinear Control*. 2022; 32(5): 2864-2882.
11. Rosa L, Cognetti M, Nicastro A, Alvarez P and Oriolo G. Multi-task cooperative control in a heterogeneous ground-air robot team. *IFAC-PapersOnLine*. 2015; 48(5): 53-58.
12. Wang DJ, Lian BW and Tang CK. UGV-UAV robust cooperative positioning algorithm with object detection. *IEEE Transactions on Intelligent Transportation Systems*. 2021; 15(7): 851-862.
13. Narváez E, Ravankar AA, Ravankar A, Emaru T and Kobayashi Y. Autonomous VTOL-UAV docking system for heterogeneous multirobot team. *IEEE Transactions on Instrumentation and Measurement*. 2021; 70: 1-18.
14. Liao JW, Li T, Mao ZH and Fei SM. Hybrid event-triggered tracking control for unmanned autonomous helicopter under disturbance and deception attacks. *ISA Transactions*. 2022; <https://doi.org/10.1016/j.isatra.2022.09.039>.
15. Ge XH, Han QL, Zhang XM and Ding DR. Dynamic event-triggered control and estimation: a survey. *International Journal of Automation and Computing*. 2021; 18(6): 857-886.
16. Liu D and Yang GH. Robust event-triggered control for networked control systems. *Information Sciences*. 2018; 459: 186-197.
17. Banno I, Azuma S, Ariizumi R and Asai T. Sparse event-triggered control of linear systems. *International Journal of Robust and Nonlinear Control*. 2023; 33(1): 134-158.
18. Shen MQ, Shen Y and Zhang GM. A new approach to event-triggered static output feedback control of networked control systems. *ISA Transactions*. 2016; 65: 468-474.
19. Li Q, Shen B, Wang ZD, Huang TW and Luo J. Synchronization control for a class of discrete time-delay complex dynamical networks: a dynamic event-triggered approach. *IEEE Transactions on Cybernetics*. 2019; 49(5): 1979-1986.
20. He HF, Qi WH, Cao JD, Cheng J and Shi KB. Observer-based adaptive sliding-mode control under dynamic event-triggered scheme with actuator and communication faults. *International Journal of Robust and Nonlinear Control*. 2022; 1-20.
21. Wang YL, Lim CC and Shi P. Adaptively adjusted event-triggering mechanism on fault detection for networked control systems. *IEEE Transactions on Cybernetics*. 2017; 47(08): 2299-2311.

22. Wang KY, Tian EG, Liu JL, Wei LN and Dong Y. Resilient control of networked control systems under deception attacks: a memory-event-triggered communication scheme. *International Journal of Robust and Nonlinear Control*. 2020; 30: 1534-1548.
23. Tian EG, Wang KY, Zhao X, Shen SB and Liu JL. An improved memory-event-triggered control for networked control systems. *Journal of The Franklin Institute*. 2019; 356(13): 7210-7223.
24. Gu Z, Shi P, Dong Y, Shen Y and Xie XP. Memory-based continuous event-triggered control for networked T-S fuzzy systems against cyberattacks. *IEEE Transactions on Fuzzy Systems*. 2021; 29(10): 3118-3129.
25. Sun Y, Xiao H, Ding D and Liu S. Secure filtering under adaptive event-triggering protocols with memory mechanisms. *ISA Transactions*. 2022; 127: 13-21.
26. Zhang H and Zheng WX. Denial-of-service power dispatch against linear quadratic control via a fading channel. *IEEE Transactions on Automatic Control*. 2018; 63(9): 3032-3039.
27. Zhang H, Qi YF, Wu JF, Fu LK and He LD. DoS attack energy management against remote state estimation. *IEEE Transactions on Control of Network Systems*. 2018; 5(1): 383-394.
28. Hu SL, Dong Y, Cheng ZH, Tian EG, Xie XP and Chen XL. Co-design of dynamic event-triggered communication scheme and resilient observer-based control under aperiodic DoS attacks. *IEEE Transactions on cybernetics*. 2021; 51(9): 4591-4601.
29. Huang L, Guo J and Li B. Observer-based dynamic event-triggered robust H_∞ control of networked control systems under DoS attacks. *IEEE Access*. 2021; 9: 145626-145637.
30. Zhao N, Shi P and Xing W. Dynamic event-triggered approach for networked control systems under denial of service attacks. *International Journal of Robust and Nonlinear Control*. 2021; 31: 1774-1795.
31. Chen P, and Sun HT. Switching-like event-triggered control for networked control systems under malicious denial of service attacks. *IEEE transactions on automatic control*. 2020; 65(9): 3943-3949.
32. Yue BF, Su MY, Jin XZ and Che WW. Event-triggered MFAC of nonlinear NCSs against sensor faults and DoS attacks. *IEEE Transactions on Circuits and Systems II: Express Briefs*. 2022; 69(11): 4409-4413.
33. Qi YW, Yu WK, Zhao XD and Xu XD. Event-triggered control for network-based switched systems with switching signals subject to dual-terminal DoS attacks. *IEEE/ACM Transactions on Networking*. 2022; 30(3): 1283-1293.
34. Xiong SX, Chen M and Wu QX. Predictive control for networked switch flight system with packet dropout. *Applied Mathematics and Computation*. 2019; 354: 444-459.
35. Raptis IA, Valavanis KP and Vachtsevanos GJ. Linear tracking control for small-scale unmanned helicopters. *IEEE Transactions on Control Systems Technology*. 2012; 20(4): 995-1010.
36. Zuo S, Song YD, Lewis FL and Davoudi A. Output containment control of linear heterogeneous multi-agent systems using internal model principle. *IEEE transactions on cybernetics*. 2017; 47(8): 2099-2109.
37. Ding YC, Liu H, Xu H and Zhong SM. On uniform ultimate boundedness of linear systems with time-varying delays and peak-bounded disturbances. *Applied Mathematics and Computation*. 2019; 349: 381-392.
38. Gu Z, Dong Y, Park JH and Xie X. Memory-event-triggered fault detection of networked IT2 T-S fuzzy systems. *IEEE Transactions on Cybernetics*. 2023; 53(2): 743-752.
39. Persis CD and Tesi P. Input-to-state stabilizing control under denial-of-service. *IEEE Transactions on Automatic Control*. 2015; 60(11): 2930-2944.
40. Su L and Ye D. Observer-based output feedback H_∞ control for cyber-physical systems under randomly occurring packet dropout and periodic DoS attacks. *ISA Transactions*. 2019; 95: 58-67.
41. Li SB, Sauter D and Xu BG. Co-design of event-triggered H_∞ control for discrete-time linear parameter-varying systems with network-induced delays. *Journal of the Franklin Institute*. 2015; 352(05): 1867-1892.

How to cite this article: H.R Zhang, S.H. Pan, T. Li, and Z.H. Mao (2023), Switching-like event-triggered tracking control for UAH/UGV systems under external disturbance and DoS attacks, *IJRNC*, 2023;00:00–00.